

PERFORMANCE OF A 16.6-METER-DIAMETER CROSS PARACHUTE
IN A SIMULATED MARTIAN ENVIRONMENT

By Reginald R. Lundstrom, Wayne L. Darnell,
and Lucille C. Coltrane

Langley Research Center
Langley Station, Hampton, Va.

Technical Film Supplement L-985 available on request.

NATIONAL AERONAUTICS AND SPACE ADMINISTRATION

For sale by the Clearinghouse for Federal Scientific and Technical Information
Springfield, Virginia 22151 - CFSTI price \$3.00

PERFORMANCE OF A 16.6-METER-DIAMETER CROSS PARACHUTE
IN A SIMULATED MARTIAN ENVIRONMENT

By Reginald R. Lundstrom, Wayne L. Darnell,
and Lucille C. Coltrane
Langley Research Center

SUMMARY

Inflation and drag characteristics of a 54.4-foot (16.6 meter) nominal-diameter cross parachute, deployed at a Mach number of 1.65 and a dynamic pressure of 12.68 lb/sq ft (607.1 N/m²), were obtained from the fourth balloon-launched flight test of the Planetary Entry Parachute Program (PEPP). These data as well as the stability characteristics of the parachute during subsonic descent are presented herein.

After deployment the parachute quickly inflated to a full condition, partially collapsed, and then gradually reinflated while undergoing rapid oscillations between over-inflation and underinflation. The oscillations began while the parachute was still at supersonic speeds and continued to low subsonic speeds well below an altitude of 90 000 feet (27.4 km). These canopy instabilities produced large cyclic variations in the parachute's drag coefficient. The average value of drag coefficient was about 0.8 to 0.9 at subsonic speeds and slightly lower at supersonic speeds. These drag coefficient values were based on the actual fabric surface area of the parachute canopy. The parachute sustained minor damage consisting of two canopy tears and abrasions and tears on the riser line. It is believed that this damage did not produce a significant change in the performance of the parachute.

INTRODUCTION

The NASA Planetary Entry Parachute Program (PEPP) was established to provide test data on several parachute configurations for entry into planetary atmospheres. Such applications require performance characteristics in a low-density environment. Large-scale flight testing of parachutes deployed behind blunt bodies at supersonic speeds was undertaken because no test facilities suitable for investigating this application existed. In addition, little confidence existed in extrapolating large-scale parachute characteristics from small-scale parachute data. The combination of parachute size, deployment Mach number, and density environment was outside the limits of applicable experience.

Flight tests which simulate conditions expected in the Martian atmosphere during parachute operation have been conducted with the use of both rocket-launched and balloon-launched spacecraft. (See ref. 1.) Modified ring-sail, disk-gap-band, and cross parachutes have been tested. References 2 to 4 present the results presently published from the rocket-launched tests, and references 5 to 7 show the data from the first three flights of the balloon-launched series.

This document describes the basic test results obtained from the fourth flight test of the balloon-launched series of the Planetary Entry Parachute Program. Specifically, the inflation, drag, and stability characteristics are presented for a 54.4-foot (16.6 meter) nominal-diameter cross parachute deployed in the wake of a 15-foot (4.6 meter) diameter spacecraft. The parachute was deployed at a Mach number of 1.65 and a dynamic pressure of 12.68 lb/ft² (607.1 N/m²). Little analysis is presented in order to expedite publication of the basic data.

A 16-millimeter motion-picture film supplement showing the parachute inflation sequence photographed from onboard cameras is available on loan.

SYMBOLS

a_l	linear acceleration along body longitudinal axis, g units (1g = 9.807 meters per second ²)
$C_{D,o}$	drag coefficient, $\frac{\text{Drag}}{q_\infty S_o}$
$(C_{D,o})_{\text{eff}}$	effective drag coefficient, $\frac{2W}{\rho_\infty S_o \dot{Z}_E^2}$
D_o	nominal diameter, $\left(\frac{4}{\pi} S_o\right)^{1/2}$, feet (meters)
g	acceleration due to gravity, feet per second ² (meters per second ²)
q_∞	free-stream dynamic pressure, pounds per foot ² (newtons per meter ²)
S_o	surface area of canopy, foot ² (meter ²)
T	tensiometer force, pounds (newtons)
t	onboard time, seconds
W	weight, pounds (kilograms)

X, Y, Z	body-axis system
X_E, Y_E, Z_E	earth-fixed axis system
ρ_∞	free-stream upper air density, slugs per foot ³ (kilograms per meter ³)
θ, ϕ, ψ	payload attitude angles relative to earth-fixed axis system, degrees
$\delta_{\text{parachute}}$	resultant pitch-yaw angle of parachute center line from local vertical, degrees
δ_{payload}	resultant pitch-yaw angle of payload center line from local vertical, degrees
δ'	angular difference between the center lines of payload and parachute, degrees

Dots over symbols denote differentiation with respect to time. Velocities, dynamic pressures, and Mach numbers are free-stream values unless otherwise noted.

PARACHUTE DESCRIPTION

The characteristics of the fully inflated parachute are as follows:

Parachute type	Cross
Nominal diameter, ft (m)	54.4 (16.6)
Actual canopy area, ft ² (m ²)	2323.4 (215.8)
Width of major and minor panels, ft (m)	18.8 (5.7)
Length of major panel, ft (m)	71.3 (21.8)
Length of each minor panel, ft (m)	26.3 (8.0)
Length of each suspension line, ft (m)	67.2 (20.5)
Number of suspension lines	64
Weight (in fig. 1, the parachute and all lines above upper tensiometer connecting point), lb (kg)	73.6 (33.4)

The configuration of the cross parachute canopy is sketched in figure 2. Each of the canopy panels were constructed from 3-foot (0.9 meter) wide strips of dacron cloth which were sewn side to side in lengths equal to the width of the panels. The minor panels were attached on either side of the major panel to form a symmetrical cross. The cloth weighed 1.25 oz/yd² (42.4 gm/m²) and had a rated breaking strength of 50 lb/in. (88 N/cm). Porosity of this fabric was 150 ft³/min/ft² (45.7 m³/min/m²) at a differential pressure of 1/2 inch (1.27 cm) of water. The canopy fabric was reinforced with

32 dacron radial tapes which were laid across the entire length of the cross, 16 running in each direction, spaced approximately 15 inches (38 cm) apart. (See fig. 2.) These tapes which were 3/4 inch (1.9 cm) wide and 0.037 inch (0.094 cm) thick were rated at 750 lb (3336 N) breaking strength. Reinforcing tapes were also sewn across each of the four ends of the cross. This skirt tape was dacron, 1 inch (2.5 cm) wide and 0.035 inch (0.088 cm) thick. The breaking strength of the skirt tape was rated at 1000 lb (4448 N). The completed parachute canopy was all white except for a 12-inch (30.5 cm) wide black stripe which ran from the apex to the edge of one panel. Also each panel was edged with a 12-inch (30.5 cm) dyed black stripe.

Figure 1 shows a sketch of the inflated cross parachute including its suspension lines and the connecting canopy bridle, two riser line sections and load bridle. The 64 suspension lines were fabricated from braided dacron cords. The rated breaking strength of each line was 550 lb (2447 N) and the line weighed 0.0055 lb/ft (0.0082 kg/m). Each set of 16 suspension lines attached to an arm of the cross and terminated at their lower end at two short branches of the canopy bridle (eight suspension lines to each short branch). Each set of two short branches converged into one of the four main canopy bridle legs and they, in turn, converged into the riser line as shown in figure 1. The material used in the canopy bridle was dacron webbing 1.719 inches (4.37 cm) wide and approximately 0.070 inch (0.178 cm) thick. This material provided a rated breaking strength at each of the short branches of the bridle of 6000 lb (26 689 N) where a single thickness was used. The combination of the eight webbing thicknesses accumulated at the final confluence point of the canopy bridle produced a total rated breaking strength of 48 000 lb (213 514 N). The eight thicknesses of webbing material gathered in the canopy bridle extended down to the upper tensiometer connection point forming the upper section of the riser line. Attached to the lower tensiometer connecting point was the lower section of the riser line. This riser section carried the load to the load bridle which was symmetrically attached to the payload at three points. Each of the three legs of the load bridle was made up of two thicknesses of dacron webbing. This webbing was somewhat thicker and heavier than that in the canopy bridle, being approximately 0.10 inch (0.25 cm) thick. The breaking strength of each thickness of this webbing was 6500 lb (28 913 N). The total rated breaking strength for the six thicknesses of webbing in the load bridle was 39 000 lb (173 480 N). The parachute was designed and built under NASA Contract NAS1-6703.

The parachute was packed to a density of 40 lb/ft³ (640 kg/m³) in a cylindrical dacron bag. The bag was lined with teflon-coated fabric to prevent abrasion. No canopy or suspension line holders or restraints were used inside the deployment bag except for a break line from the apex of the canopy to the top of the bag. Also attached to the top of the bag was a mortar lid and steel ballast. The combined weight of the deployment bag, mortar lid, and ballast was approximately 6 lbm (2.7 kg).

The packed parachute (not including the bridle, tensiometer, mortar lid and ballast) was subjected to a heating process as part of a proposed sterilization procedure for equipment which may be used in interplanetary atmospheric entry missions. The parachute was exposed to a temperature of 125° C for 38 hours including about 30 hours required to bring all parachute material up to the test temperature. The parachute was subjected to this high-temperature environment so that any resulting material degradation would exist during the flight test. Proposed sterilization procedures for a Mars mission would have required 90 hours at 125° C instead of 38 hours.

TEST SYSTEM DESCRIPTION

The spacecraft used for this test was 15 feet (4.6 meters) in diameter (see fig. 3) and was lifted to an altitude near 130 000 ft (39 624 m) by a 26 000 000 ft³ (736 000 m³) balloon system. The balloon system was designed and launched by the U.S. Air Force Cambridge Research Laboratories. The principal components of the spacecraft were an aeroshell, the payload, and the test parachute.

Onboard instrumentation included five motion-picture cameras, four accelerometers, and a tensiometer. Camera 1 had a frame rate of approximately 350 frames per second and viewed the parachute inflation. Cameras 2 and 3 ran at 16 frames per second. Camera 2 was used to determine payload motions from photographs of the horizon. Camera 3 photographed the inflation process and the parachute motions until about 150 seconds after payload separation. The aeroshell cameras (cameras 4 and 5) ran at 64 frames per second and photographed both the parachute inflation and payload separation from the aeroshell. Deceleration loads were recorded on ±5g and ±50g longitudinal accelerometers located in the payload. Normal and transverse accelerometers (±1g) were also positioned in the payload. A tensiometer (0 to 20 000 lb) (0 to 89 000 N) was located in the parachute riser line. All accelerometer and tensiometer data were recorded by an onboard tape recorder. The tape recorder and cameras were recovered from the payload and aeroshell after impact. Both the aeroshell and payload contained radar tracking beacons in addition to recovery beacons which aided in recovery operations. Radar and optical tracking data were provided by the White Sands Missile Range.

The aeroshell was a 120° total-angle blunted cone with a base diameter of 15 ft (4.6 m). Its construction was similar to that described in reference 8 except that eight Titan IIC staging rocket motors were substituted in place of the 12 rocket motors used in that test. The purpose of this modification was to provide deployment at supersonic velocities instead of at transonic conditions.

The payload configuration was essentially a cylinder 3.26 ft (0.994 m) in length and 1.75 ft (0.534 m) in diameter with a ballast attached at the bottom. (See fig. 3.)

Mass properties of the suspended payload were:

Weight, lb (kg)	491.9 (223.13)
Center of gravity, ft (m)	0.98 (0.30)
Pitch inertia, slug-ft ² (kg-m ²)	45.02 (61.06)
Yaw inertia, slug-ft ² (kg-m ²)	44.70 (60.62)
Roll inertia, slug-ft ² (kg-m ²)	5.02 (6.80)

These payload data were computed on the total mass suspended under the descending parachute from the upper connecting pin of the tensiometer to the bottom of the payload. The payload center of gravity was measured longitudinally from the interface between the cylinder and the ballast; positive direction is up toward the parachute. The load bridle was attached to the payload at three points. These load bridle attachment pins were located radially 0.66 foot (0.20 m) from the longitudinal axis and 120° apart. The plane of these attachment pins is located 2.24 feet (0.682 m) above the center of gravity of the suspended payload.

The cross parachute was packed into a cylindrical dacron bag and inserted into a mortar tube. The mouth of the bag rested on a sabot (ejection piston) at the bottom of the mortar. The mortar cover, which was fastened to the bottom of the bag, closed the mortar and held the packed parachute in place. The mortar, which was approximately 12 inches (30.5 cm) in diameter and 31 inches (78.7 cm) in length, was designed to eject the packed parachute at an initial relative velocity of 130 ft/sec (39.6 m/sec). A circular knife located on the parachute riser was used to cut the parachute bag mouth tie immediately after the bag was ejected from the mortar. The parachute was packed so that the suspension lines deployed before the canopy. When the suspension lines were fully extended, the combined momentum of the mortar cover, ballast, and parachute bag served to pull the parachute canopy out of the bag.

The payload was secured inside the aeroshell, prior to deployment, by an explosive nut. Approximately a half-second after mortar fire, the explosive nut was ignited in order to allow separation of the two items. When the parameter

$$\frac{\text{Parachute drag} - \text{Friction between payload and aeroshell}}{\text{Total payload weight}} \text{ exceeded } \frac{\text{Aeroshell drag}}{\text{Aeroshell weight}}$$

the payload was extracted from the rear of the aeroshell and flew a different trajectory from the aeroshell. The mission profile is shown in figure 4.

TEST ENVIRONMENT

The balloon-spacecraft system was launched from Walker Air Force Base, Roswell, New Mexico, on August 22, 1967, by using the balloon-launch technique described in reference 8. About 3½ hours after launch the system had reached 129 000 feet (39 000 m)

altitude and had drifted over the desired release point at White Sands Missile Range, New Mexico. Approximately 4.0 seconds after spacecraft release at 10:24 m.d.t., the rocket motors ignited and subsequently propelled the spacecraft to supersonic velocities. The mortar fired at 7.7 seconds after release, which ejected the parachute bag and initiated the parachute deployment. The data period for parachute testing began at this time and extended until $t = 170$ seconds.

Atmospheric soundings were made by Arcasonde rockets in the vicinity of the flight-test area. One was launched $3\frac{1}{2}$ hours before the flight test and another was launched 30 minutes before. The pressure and density data obtained from the Arcasonde rocket launched 30 minutes before the flight test appeared to be incorrect but the wind data were valid and are used in this report. Pressure and density data from an Arcasonde rocket launched the following day agreed very well with that obtained from the Arcasonde launched $3\frac{1}{2}$ hours before the flight test. Since these two data varied only slightly about the established data given in table 5.1 of the U.S. Standard Atmosphere Supplements, 1966 (month of July at latitude 30° N), the established data were accepted as the best representation of the soundings and are used in this report. (See ref. 9.) Atmospheric density and pressure data obtained from the applicable table in the U.S. Standard Atmosphere Supplements, 1966, are presented in figures 5 and 6, respectively. Data points from the two Arcasonde soundings are included in the figures and the 1962 standard atmosphere values are shown as a matter of interest. The wind velocity and direction data taken 30 minutes before the flight test are shown in figure 7.

Radar and/or optical tracking data were obtained on the payload throughout the flight. The payload's trajectory during the prime test period is shown in figure 8. Altitude- and velocity-time histories and Mach number and dynamic-pressure variations are shown in figures 9 and 10, respectively, for the test period. Velocity data presented in this report from 7.7 to 10.5 seconds represent the combined results of radar, optical, and integrated accelerometer data. Where comparisons could be made, the agreement between the three methods was good. All velocity data shown in this report are true airspeed. (They have been corrected for wind effects.) Figure 11 presents the velocity, Mach number, and dynamic-pressure histories during the prime data period.

PARACHUTE PERFORMANCE

The primary objective of the flight test was to determine inflation, drag, and stability characteristics for the 54.4-foot (16.6 meter) diameter cross parachute. For convenience, each characteristic is discussed separately. A 16-millimeter motion-picture supplement L-985 showing the parachute inflation is available on loan. A request card for the film can be found at the back of this document.

Inflation Characteristics

The deployment sequence was initiated by the mortar firing the packed parachute rearward from the payload. Mortar fire occurred at a Mach number of 1.65 and a dynamic pressure of 12.7 lb/sq ft (607.1 N/m²). The suspension lines were strung out, line stretch occurred, and then the canopy began to emerge from the bag. When the canopy was completely pulled out of the weighted parachute bag, the bag continued rearward while the parachute opened to a fully inflated condition. During the inflation process the parachute developed sufficient drag to pull the payload from the aeroshell hub. The parachute canopy reached full inflation very quickly, and then partially collapsed. This condition was followed by a gradual process of reinflation characterized by an overriding series of canopy oscillations between increased inflation and partial collapse. The high drag force on the parachute during full inflation caused it to be swept back into the path of the empty parachute bag with the weighted mortar lid attached. These items tore through the canopy in an area adjacent to the crossover area.

Times for significant events during parachute inflation were as follows:

Event	Onboard time, sec	Time from mortar fire, sec
Mortar fire	7.70	0
Line stretch	8.41	.71
Estimated bag strip	8.87	1.17
Payload separation	9.02	1.32
Full inflation	9.09	1.39
Parachute bag collision	9.26	1.56

Photographs of the parachute inflation taken at 16 frames per sec by the payload camera (camera no. 3) are presented in figure 12. Figure 12(a) shows three frames during the initial inflation sequence. Figure 12(b) shows growth to full inflation. Figure 12(c) shows the partial collapse and subsequent reinflation. It is believed that this partial collapse and reinflation process represents the response of the flexible parachute and suspension line system to the rapidly applied initial load.

Inflation loads were measured by the two longitudinal accelerometers and the tensiometer and are presented in figures 13 and 14. The significant events recorded by these instruments from mortar firing to the time of initial full inflation of the canopy are indicated in each figure. Growth of the parachute canopy projected area during inflation is depicted in figure 15. This figure compares the projected canopy area at a time t with that at 9.09 seconds when initial full inflation occurred. Partial collapse at 9.27 seconds was followed by a long series of oscillations which show a gradual growth

in mean value of parachute projected area. The mean value eventually exceeds that at full inflation, which possibly indicated a change in the effective projected canopy diameter due to the decreasing Mach number and dynamic pressure. Stable inflation was not attained during the test period (≈ 160 sec).

Drag Characteristics

Drag characteristics for the parachute-payload system during deceleration through the Mach number range (prior to apogee) were determined by use of accelerometer and tensiometer data, from accelerometer results,

$$C_{D,o} = \frac{-W_{\text{total}} a_z}{q_{\infty} S_0}$$

and by using tensiometer data

$$C_{D,o} = \frac{W_{\text{total}}}{W_{\text{payload}}} \frac{T}{q_{\infty} S_0}$$

The weight of the total descending parachute-payload system W_{total} was 565.5 lb (257.08 kg) and the weight of the payload (W_{payload}), including the load bridle but not including parachute or tensiometer, was 483.8 lb (219.45 kg). Figure 16 shows the variation of $C_{D,o}$ with Mach number by using both accelerometer and tensiometer data. Large fluctuations in the canopy shape have produced the large rapid $C_{D,o}$ oscillations. The trend is indicated by the curve faired through the oscillations. In the subsonic region the average value of $C_{D,o}$ is estimated to be about 0.8 to 0.9 and slightly lower at supersonic speeds. Estimated uncertainty for the value of $C_{D,o}$ in figure 16 is ± 0.04 . The uncertainty is based on a first-order analysis, 3-percent velocity error, 3-percent density error, and 1-percent accelerometer and tensiometer error being assumed.

Values for the "effective" drag coefficient based on vertical descent velocity were calculated by using the following equation:

$$(C_{D,o})_{\text{eff}} = \frac{2 \left(W_T - \frac{W_T}{g} \ddot{z}_E \right)}{\rho_{\infty} S_0 \dot{z}_E^2}$$

Variation of $(C_{D,o})_{\text{eff}}$ with altitude is shown in figure 17. The amount of uncertainty indicated is based on 3-percent errors in both descent velocity and density. The data of figures 16 and 17 indicate that the cross parachute produced a relatively high drag coefficient for the Mach number and dynamic-pressure range of the test.

Stability Characteristics

Stability characteristics of the descending parachute system were determined from both trajectory and camera data. Photographs from camera 2 (fig. 3) viewing the horizon were analyzed by using the methods of reference 10 extended to the conditions of this test. Attitude angles of the payload relative to the local horizon were obtained. The body-axis and Euler angle systems shown in figure 18 were used for ease of data reduction. The angle ψ is the azimuth of the body X-axis, and θ and ϕ are measures of the pitching and yawing motions. The resultant angle δ_{payload} is the total pitch-yaw displacement of the longitudinal axis from the local vertical. Time histories of θ , ϕ , and δ_{payload} depicting the pitching and yawing motions of the payload are shown in figure 19. These data are estimated to be accurate within 3° . Figure 20 shows δ_{payload} as a function of altitude. The wide variations of δ_{payload} with altitude indicate the large swinging amplitudes of the payload throughout this range of descent altitudes. Very little damping is evident. Although some of these swinging motions can be attributed to wind-shear effects, it is believed that such motions above 125 000 feet (38.1 km) were produced mainly by large fluctuations in canopy shape as mentioned previously.

Observation of the camera 3 film indicated that relative motions existed between the payload and the parachute which reached a maximum shortly before apogee (18.4 sec), and diminished slowly during descent. For this reason the payload values of θ , ϕ , and δ_{payload} shown in figure 19 should not be considered necessarily representative of parachute angular motions. Figure 21 shows three curves which illustrate the relationship of the payload and parachute motions for a portion of the early descent. The uppermost curve δ_{payload} presents the total pitch-yaw displacements of the payload longitudinal axis relative to the local vertical, shown previously in figure 20. The middle curve of figure 21 $\delta_{\text{parachute}}$ depicts the total pitch-yaw displacement of the parachute's longitudinal center line from the local vertical. The bottom curve of this figure δ' shows the angular difference between the center line of the payload and the parachute. Ground-based telescope tracking film revealed that the payload-parachute motions continued sporadically for many minutes of the descent (above 90 000 ft (27.4 km)). The film showed that the payload was swinging outward and around while the parachute was rotating and rocking. The canopy was scissoring and pulsating. At this same time the payload was turning under the parachute, twisting and untwisting the riser lines and, to some extent, the bridles. At altitudes below ≈ 90 000 feet (27.4 km), the canopy achieved stability for short periods but remained subject to periodic instabilities, perhaps caused by wind-shear layers. Because of the extremely high pitching and yawing motions developed after initial full inflation and continuing into early descent, the stability characteristics of the parachute were considered to be very poor.

PARACHUTE STRUCTURAL DAMAGE

After recovery the parachute was inspected for damage. The parachute canopy sustained damage in two areas which occurred during the test portion of the flight. A large tear was found on one of the panels immediately adjacent to the crossover area. The tear formed a T-shape; the top of the T extended along a radial tape located about a third of the way in from one of the side edges and was about 34 inches (86.2 cm) long. The tear forming the stem of the T was about 14 inches (36 cm) long. Motion pictures show that this tear occurred when the mortar lid and parachute bag penetrated the parachute canopy. A small tear was found in the crossover area of the canopy near the apex. This tear was nearly circular and approximately 3 inches (7.6 cm) in diameter. Although the cause of this tear is not definitely known, it is likely that it was produced by one of many pieces of debris which were blown out with the parachute bag. The canopy penetration from such an item would probably occur in the same manner as that of the mortar lid and parachute bag.

A photograph of the damaged parachute canopy taken by camera 3 during the early part of descent is shown in figure 22. A third area of damage was discovered after recovery. This damage was confined to the canopy bridle and connecting riser webbing. The becket (webbing loop) which constrained the knife to cut the parachute bag tie was torn off. The riser line to the canopy bridle keeper, which constrained the canopy bridle at its confluence point (fig. 1), was torn off. All hand stitching positioning the riser webbing was broken and four of the eight webs sustained 4- to 10-inch (10 to 25 cm) tears longitudinally. The torn bridle keeper and riser stitching allowed the riser webbings to separate and caused the effective canopy bridle confluence point to move down to the upper tensiometer connecting pin and extended the length of the bridle legs an additional 5 feet (1.5 meters) to approximately 8.5 feet (2.6 meters). This damage appears to have occurred about the time of initial full inflation according to the camera 3 film.

Since the tears in the canopy represent only about 0.10 percent of the total canopy area and because it is believed that the separated webbings in the riser line did not allow the bridle legs to shift independently, it is believed that the parachute performance was little affected by any of the damage.

CONCLUDING REMARKS

Inflation, drag, and stability characteristics of a 54.4-foot (16.6 meter) nominal-diameter cross parachute were obtained from the fourth flight of the balloon-launched series of the Planetary Entry Parachute Program. Deployment occurred at a Mach number of 1.65 and a dynamic pressure of 12.68 lb/sq ft (607.1 N/m²). After deployment the parachute quickly inflated to a full condition, partially collapsed, and then

gradually reinflated while undergoing rapid oscillations between overinflation and underinflation. These oscillations plus localized flexuring of the canopy began while the parachute was still at supersonic speeds and continued to low subsonic speeds well below an altitude of 90 000 feet (27.4 km). The excessive canopy instabilities produced large cyclic variations in the drag coefficient of the parachute. The average drag coefficient developed was about 0.8 to 0.9 at subsonic speeds and slightly lower at supersonic speeds. Drag coefficient values were based on the actual fabric surface area of the parachute canopy. During the reflation process, the parachute bag and attached mortar lid and weight collided with the canopy and caused a tear in one panel. In addition, the upper riser line webbings were separated but neither of these damaged areas appeared to have a significant effect on parachute performance.

Langley Research Center,
National Aeronautics and Space Administration,
Langley Station, Hampton, Va., February 19, 1967,
709-08-00-01-23.

REFERENCES

1. McFall, John C., Jr.; and Murrow, Harold N.: Parachute Testing at Altitudes Between 30 and 90 Kilometers. AIAA Aerodynamic Deceleration Systems Conference, Sept. 1966, pp. 116-121.
2. Preisser, John S.; Eckstrom, Clinton V.; and Murrow, Harold N.: Flight Test of a 31.2-Foot-Diameter Modified Ringsail Parachute Deployed at a Mach Number of 1.39 and a Dynamic Pressure of 11.0 Pounds Per Square Foot. NASA TM X-1414, 1967.
3. Eckstrom, Clinton V.; and Preisser, John S.: Flight Test of a 30-Foot-Nominal-Diameter Disk-Gap-Band Parachute Deployed at a Mach Number of 1.56 and a Dynamic Pressure of 11.4 Pounds Per Square Foot. NASA TM X-1451, 1967.
4. Eckstrom, Clinton V.; Murrow, Harold N.; and Preisser, John S.: Flight Test of a 40-Foot-Nominal-Diameter Modified Ringsail Parachute Deployed at a Mach Number of 1.64 and a Dynamic Pressure of 9.1 Pounds Per Square Foot. NASA TM X-1484, 1967.
5. Whitlock, Charles H.; Bendura, Richard J.; and Coltrane, Lucille C.: Performance of a 26-Meter-Diameter Ringsail Parachute in a Simulated Martian Environment. NASA TM X-1356, 1967.
6. Bendura, Richard J.; Huckins, Earle K., III; and Coltrane, Lucille C.: Performance of a 19.7-Meter-Diameter Disk-Gap-Band Parachute in a Simulated Martian Environment. NASA TM X-1499, 1968.
7. Whitlock, Charles H.; Henning, Allen B.; and Coltrane, Lucille C.: Performance of a 16.6-Meter-Diameter Modified Ringsail Parachute in a Simulated Martian Environment. NASA TM X-1500, 1968.
8. Darnell, Wayne L.; Henning, Allen B.; and Lundstrom, Reginald R.: Flight Test of a 15-Foot-Diameter (4.6-Meter) 120° Conical Spacecraft Simulating Parachute Deployment in a Mars Atmosphere. NASA TN D-4266, 1967.
9. Anon.: U.S. Standard Atmosphere Supplements, 1966. Environ. Sci. Serv. Admin., NASA, and U.S. Air Force.
10. Anon.: Manual of Photogrammetry. Sec. ed., American Soc. Photogrammetry, c.1952.

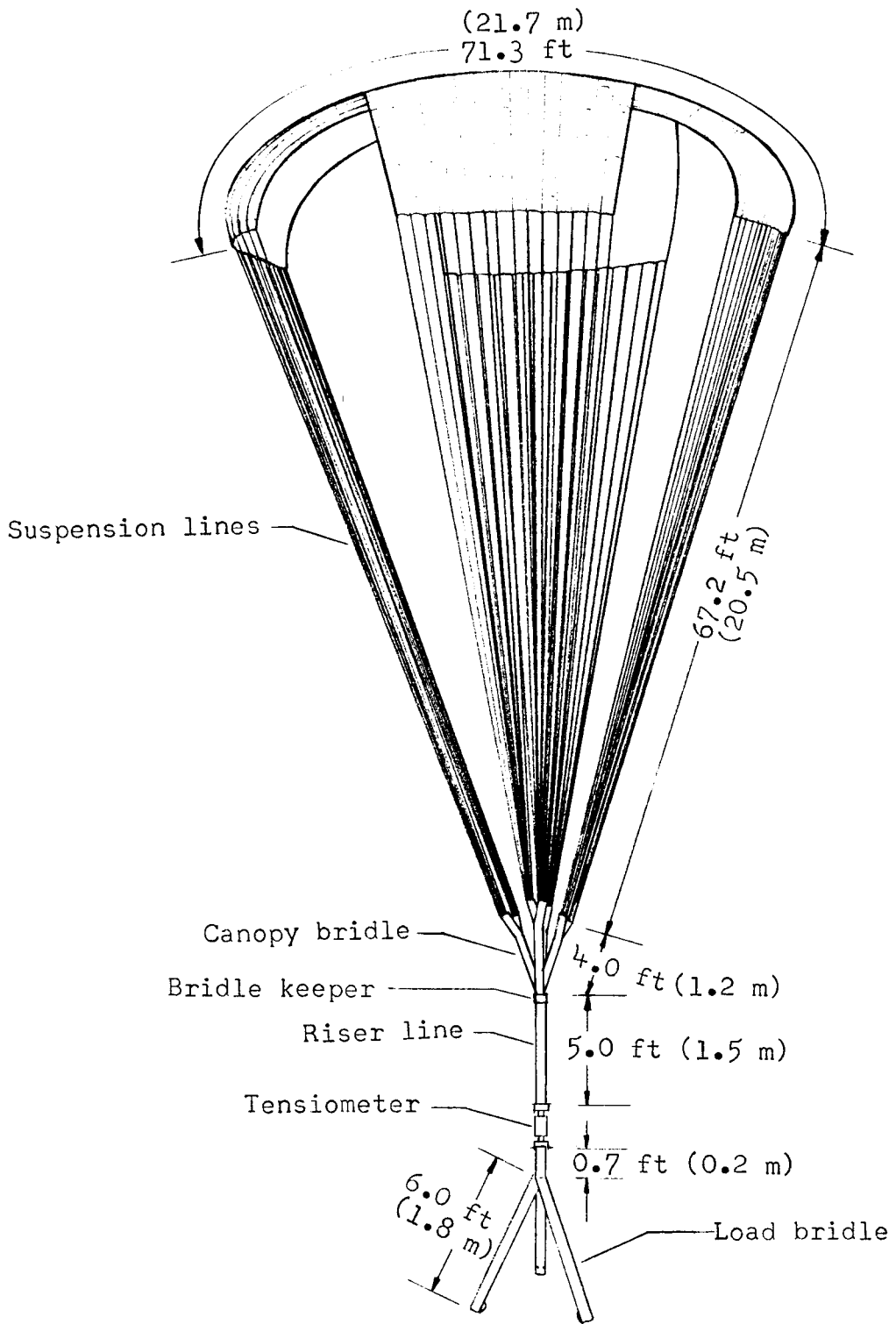


Figure 1.- Sketch of cross parachute and connecting lines. Dimensions are not drawn to scale.

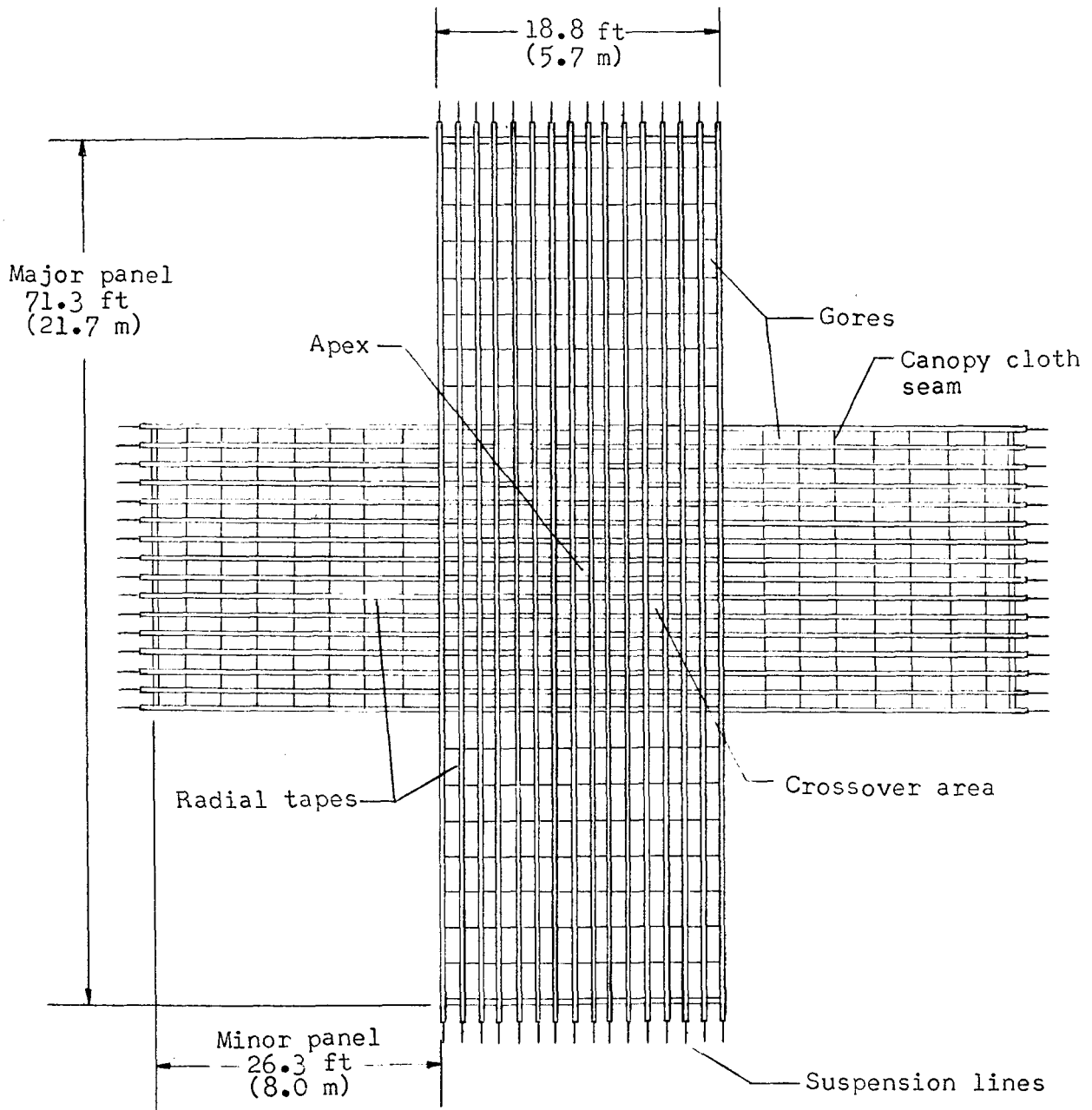


Figure 2.- Sketch of cross parachute canopy configuration. Dimensions are not drawn to scale. Crossover area is the total area in canopy center where radial tapes cross one another.

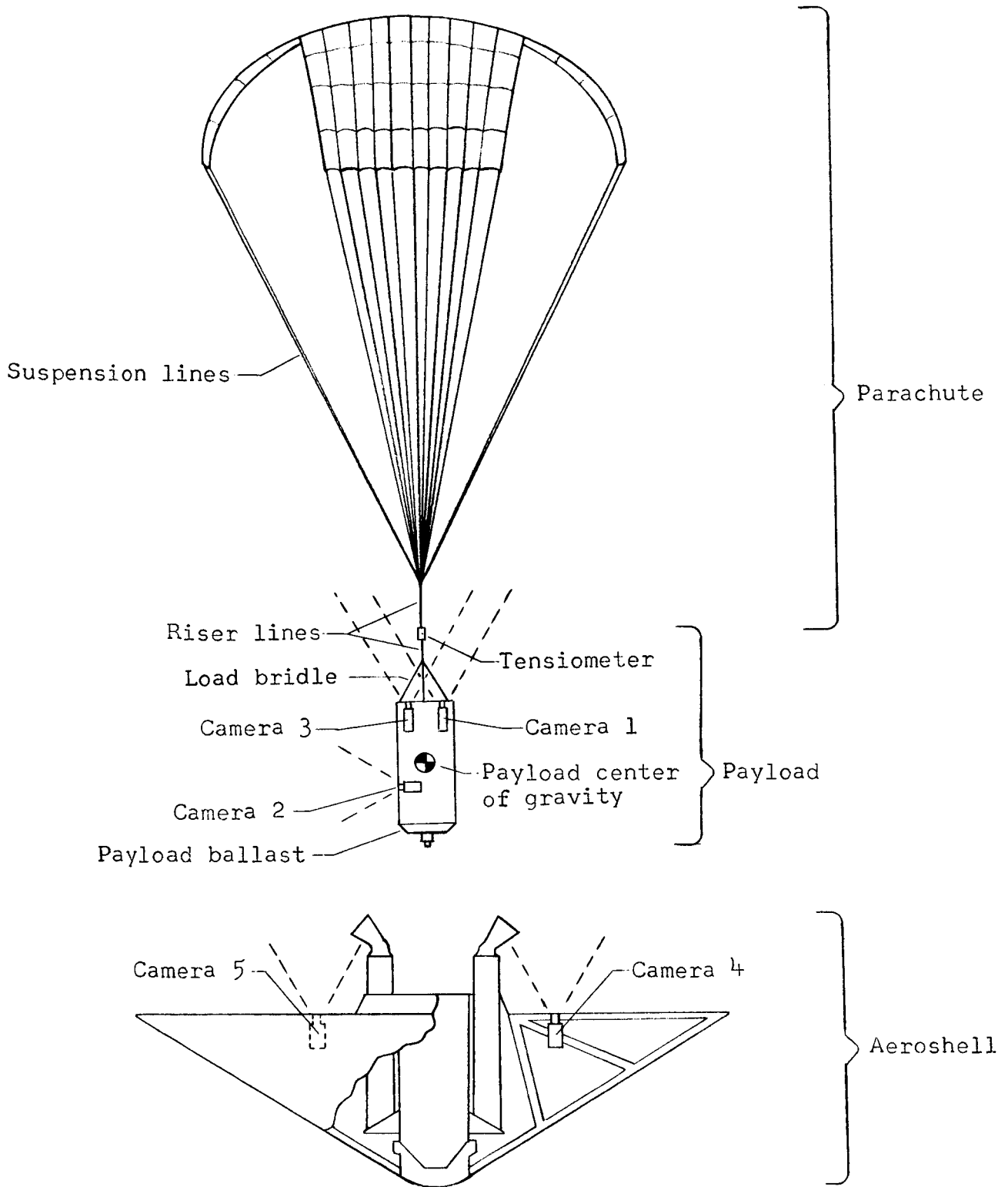


Figure 3.- Sketch of spacecraft components.

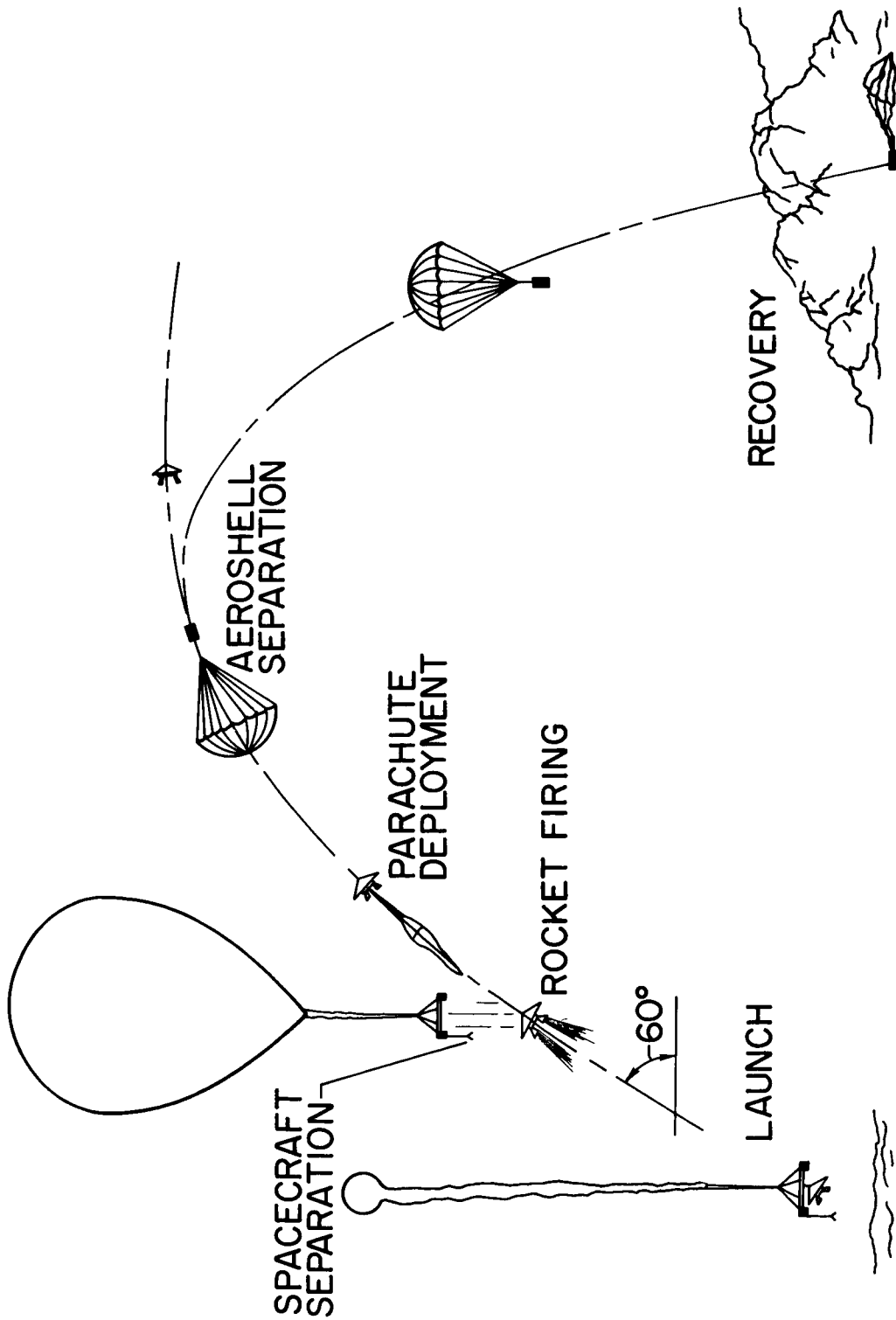


Figure 4.- Sequence of events.

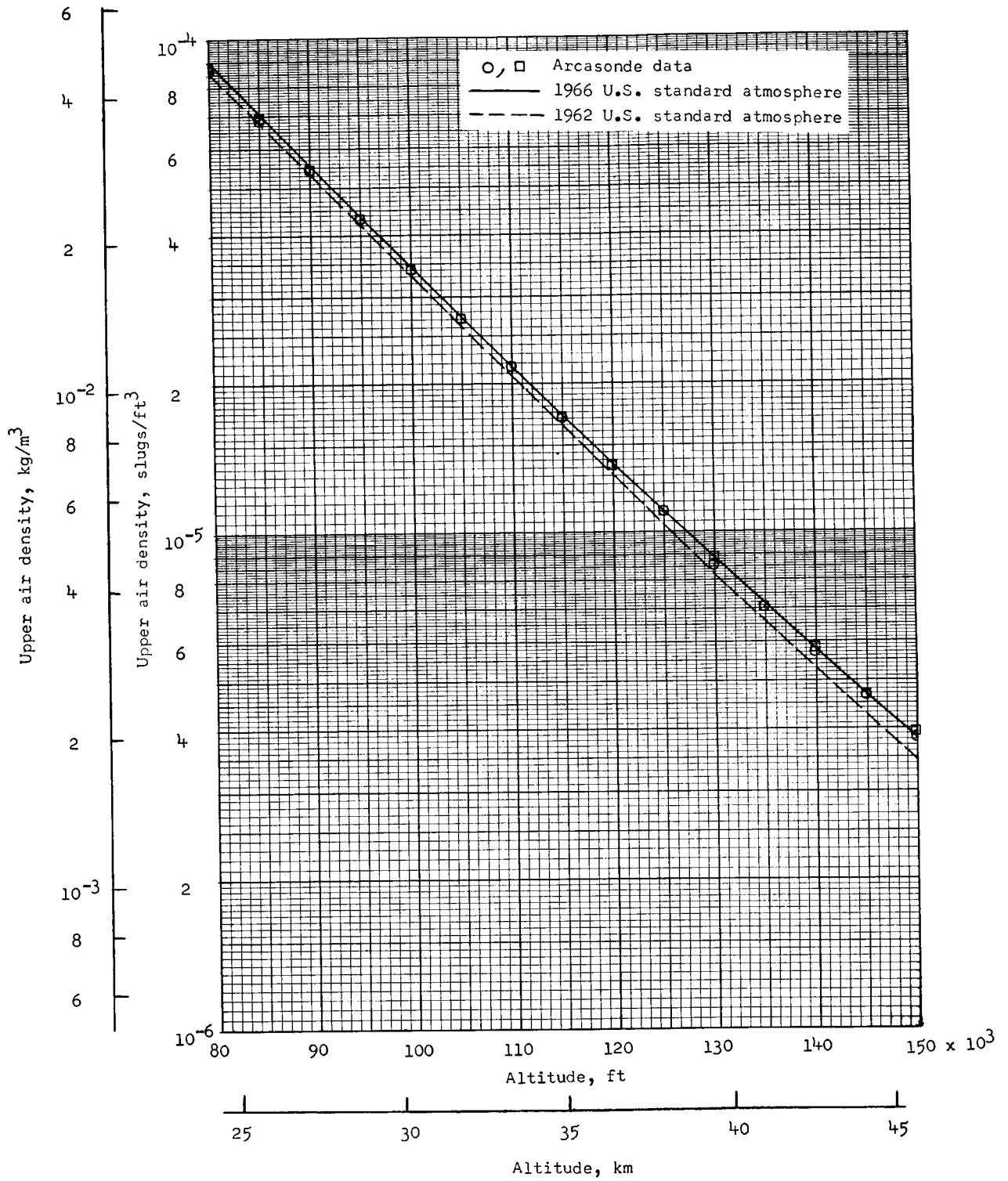


Figure 5.- Atmospheric density.

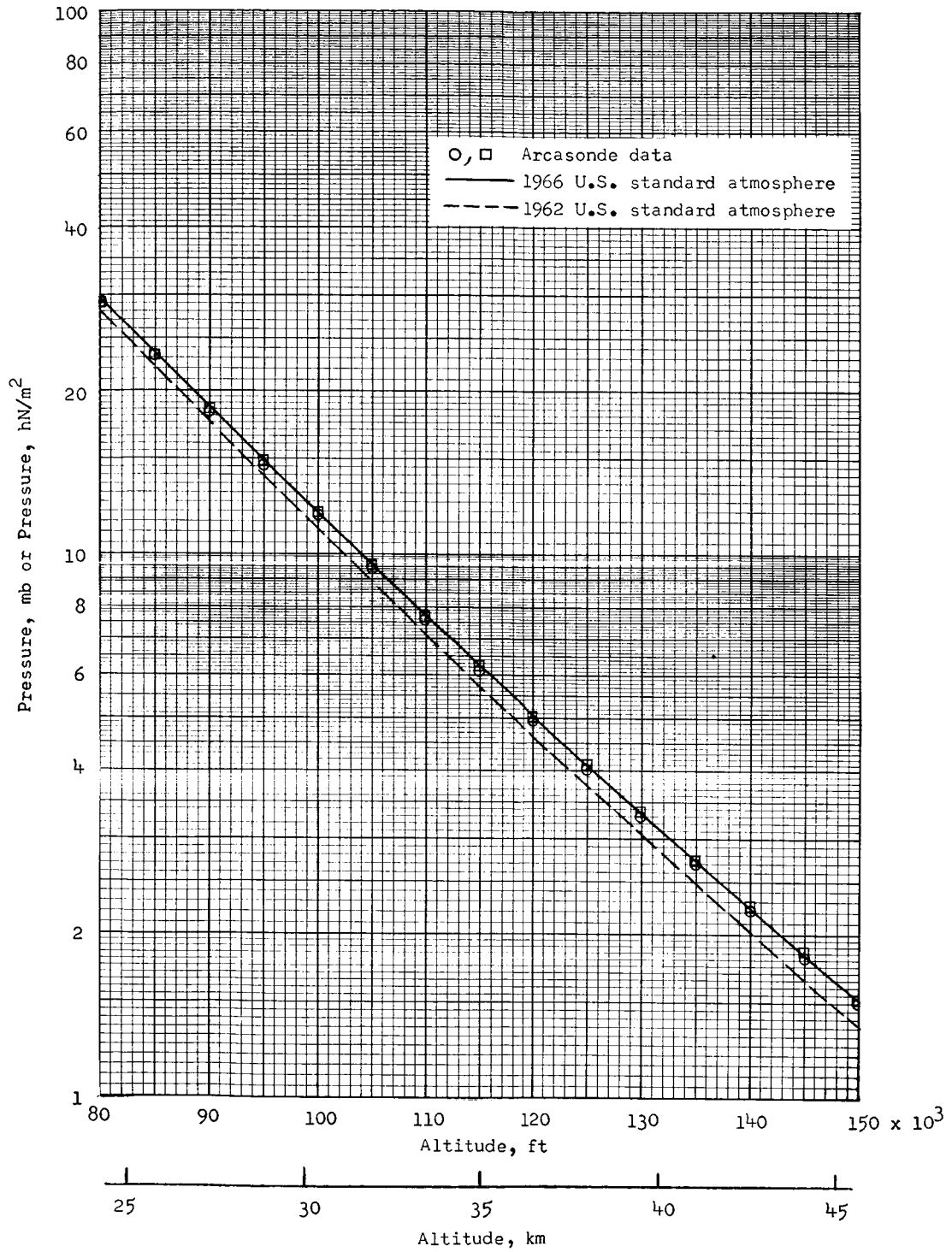


Figure 6.- Atmospheric pressure.

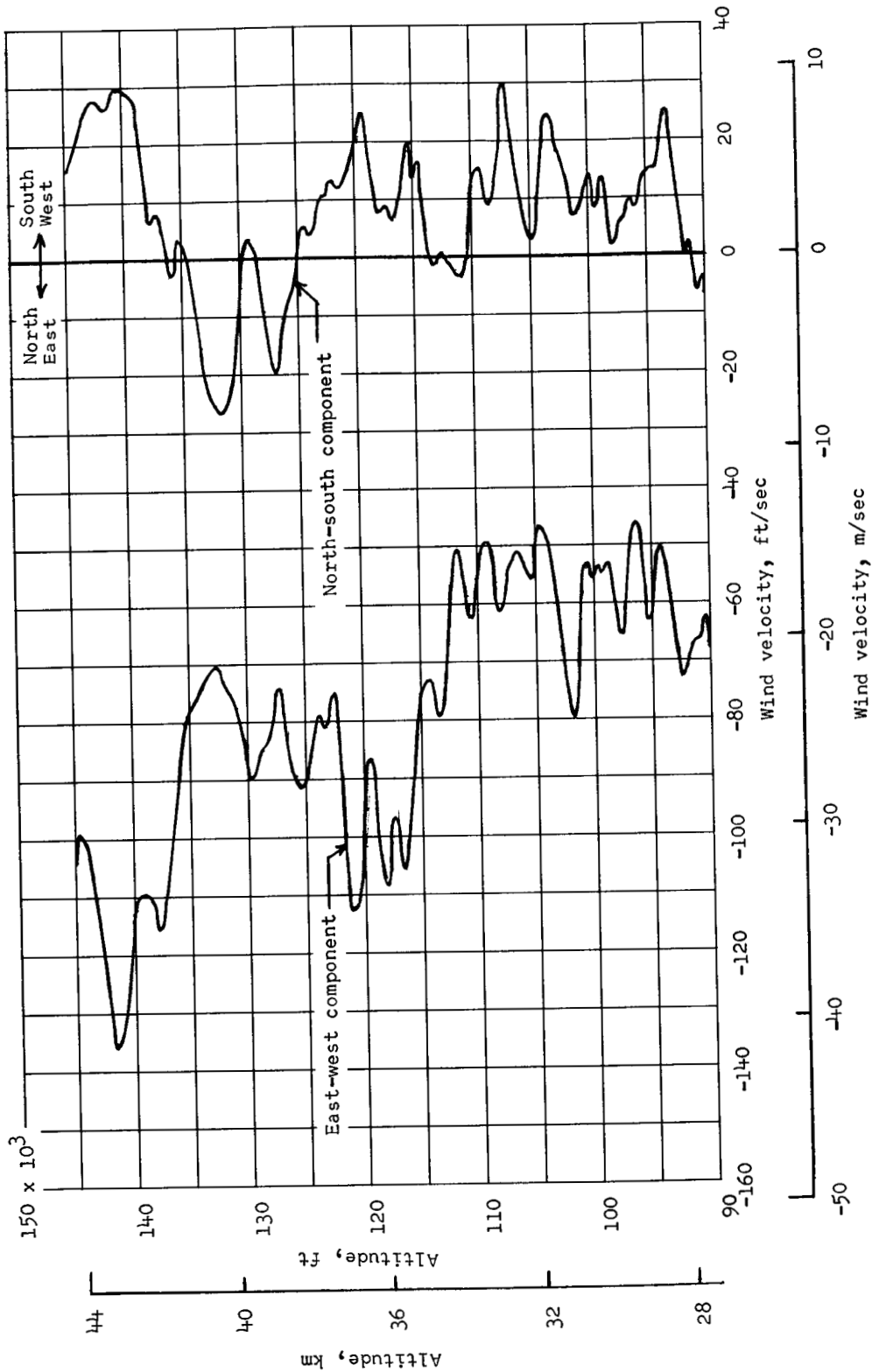


Figure 7.- Wind-velocity profile in east-west and north-south components.

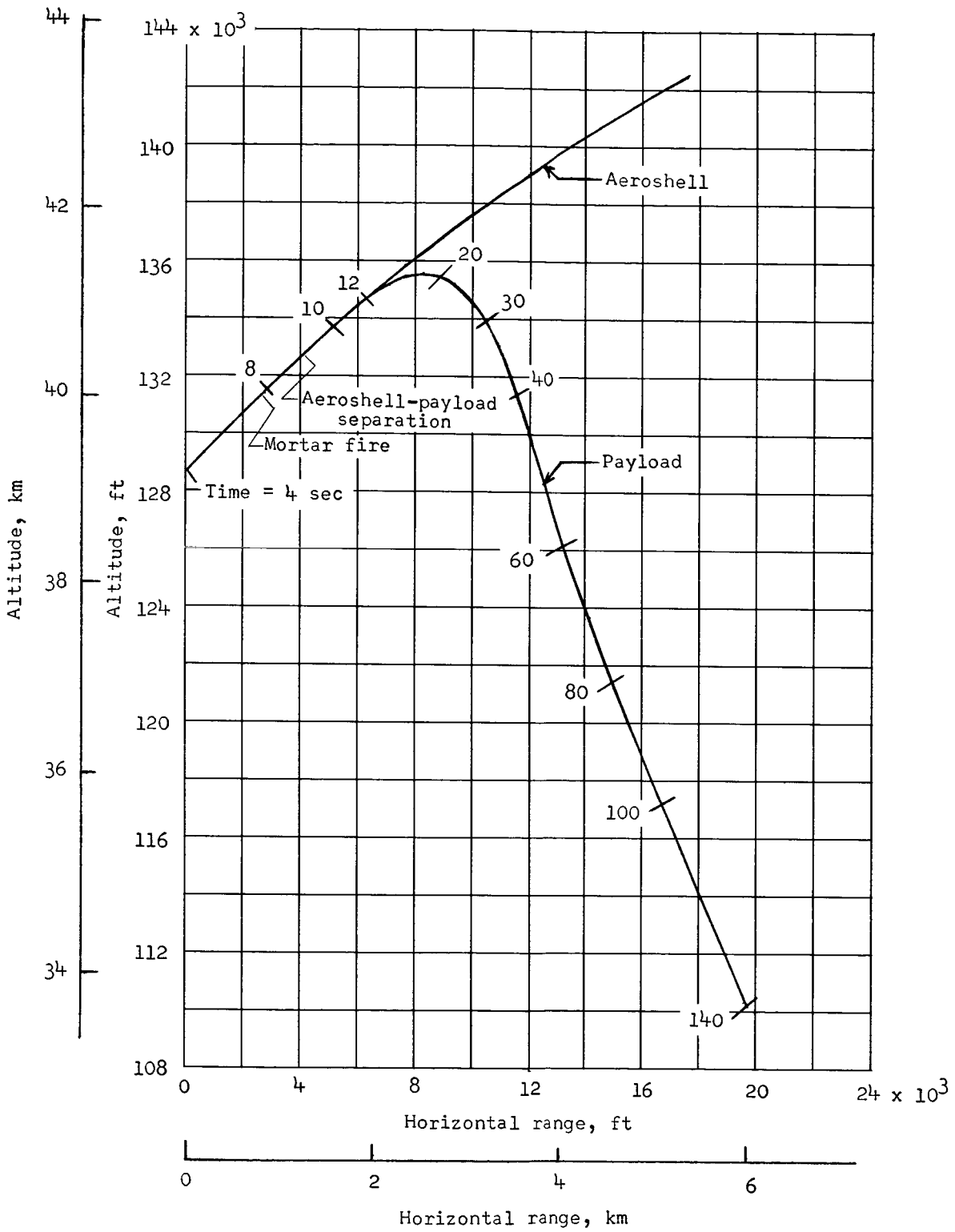


Figure 8.- Variation of altitude with horizontal range.

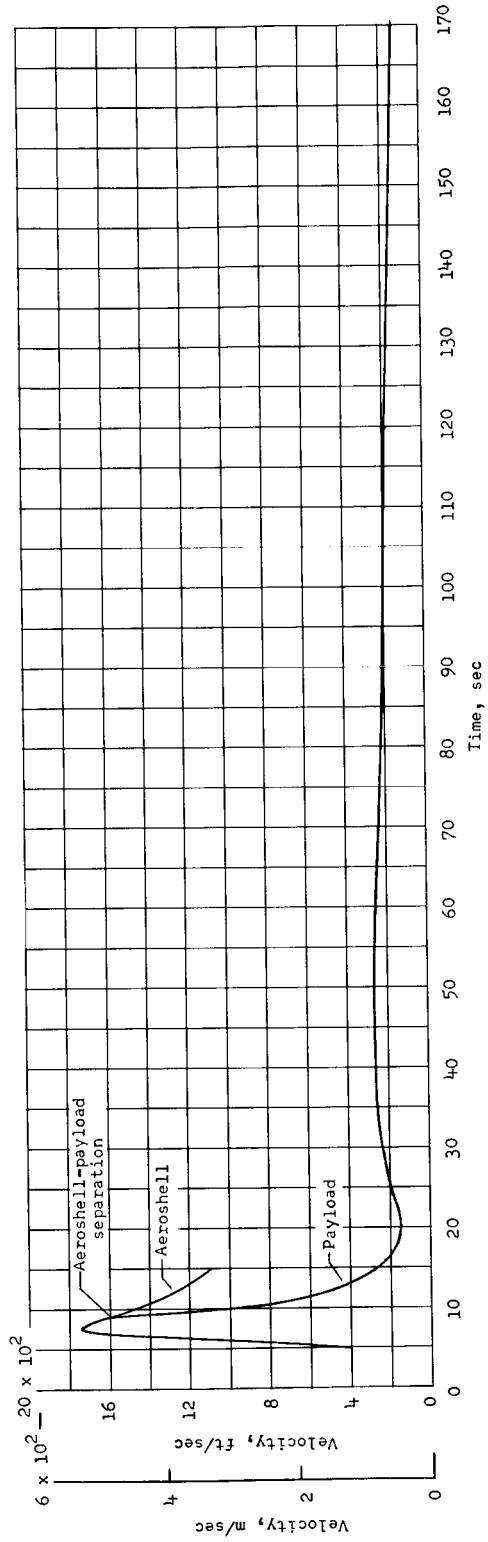
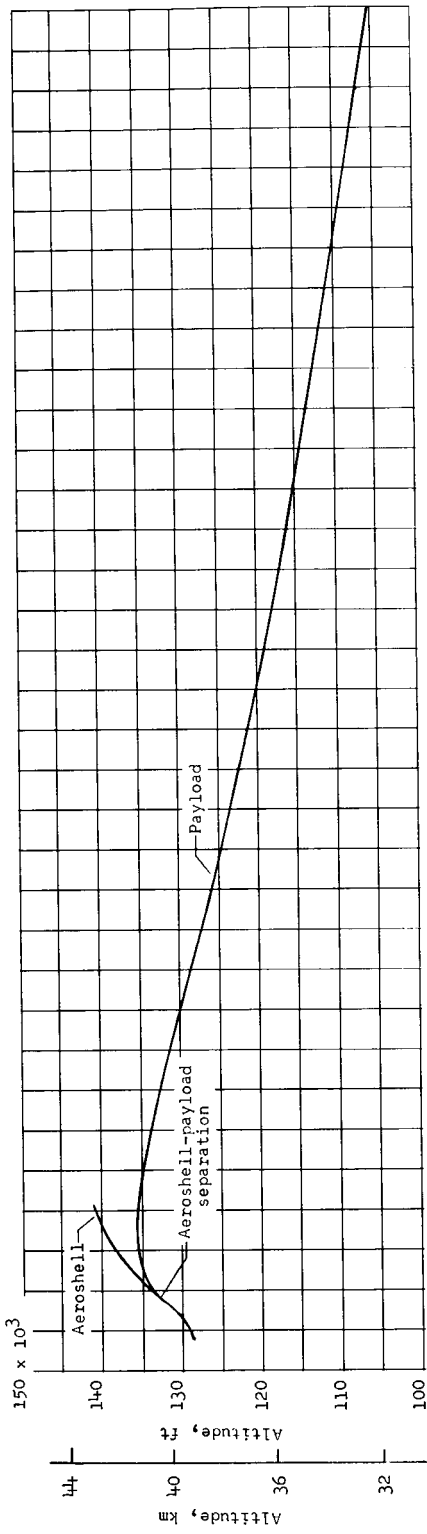


Figure 9.- Variation of altitude and velocity with time.

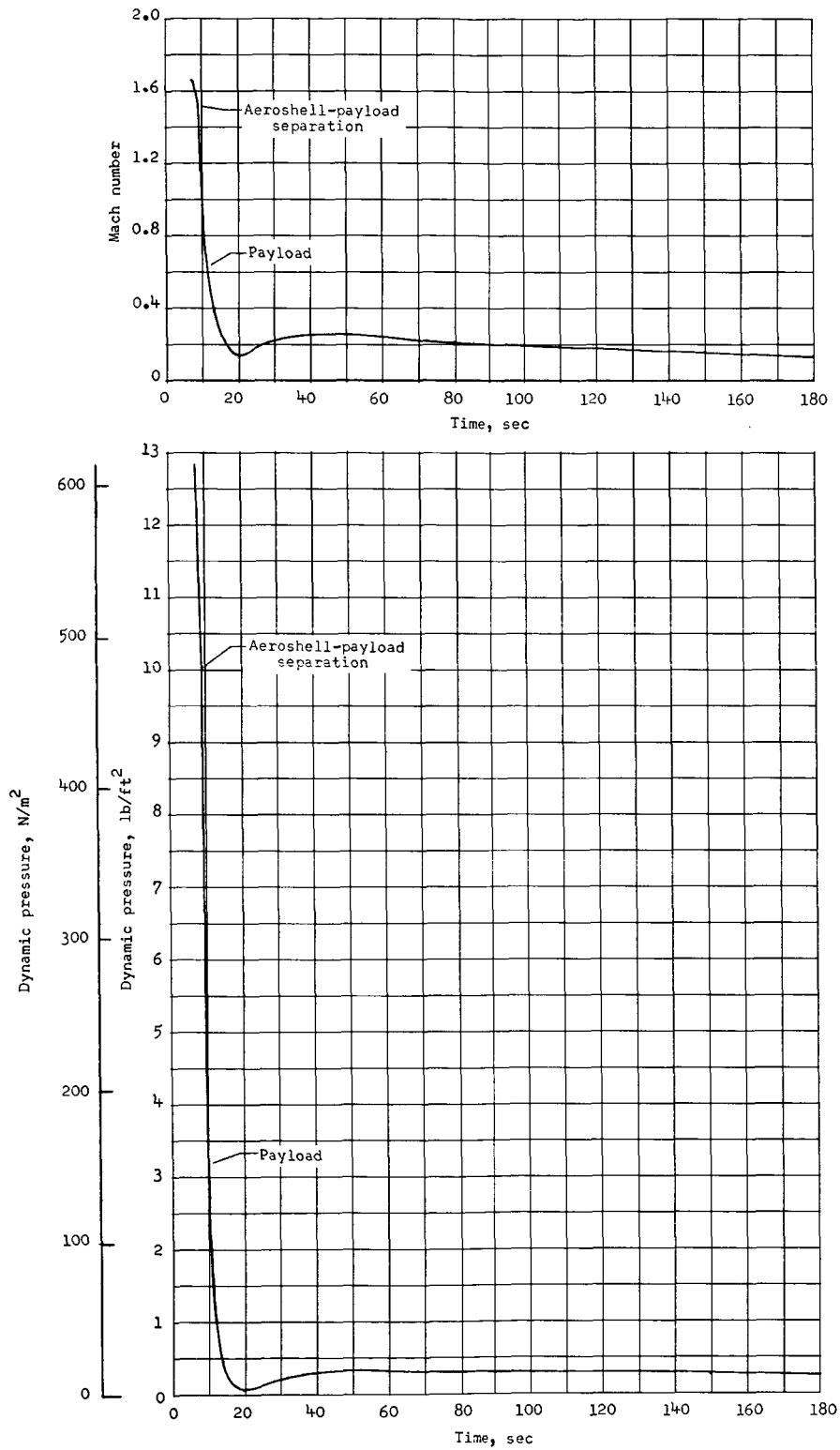


Figure 10.- Variation of Mach number and dynamic pressure with time.

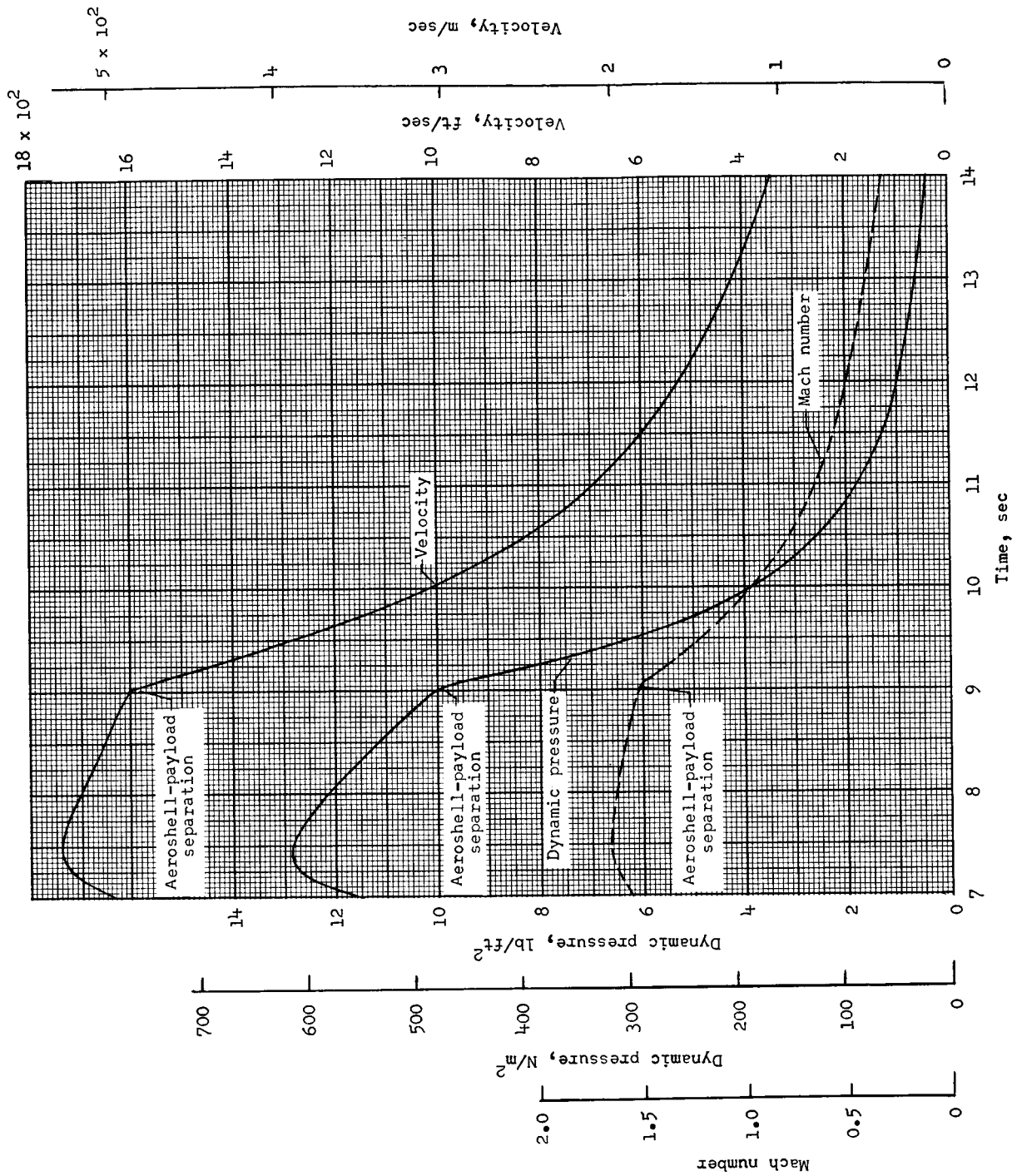
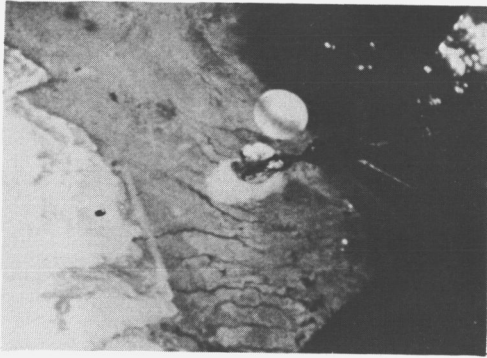
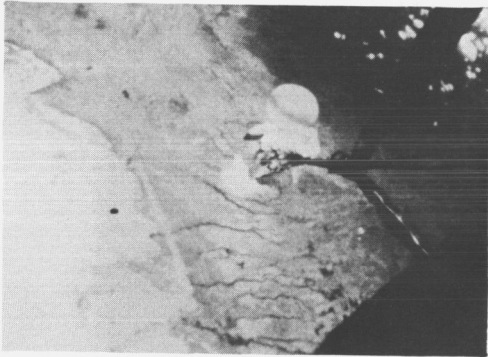


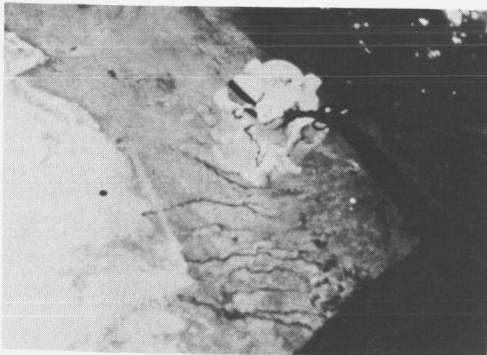
Figure 11.- Variation of velocity, dynamic pressure, and Mach number with time during parachute deployment.



Time = 8.59 seconds



Time = 8.72 seconds



Time = 8.84 seconds

(a) Beginning of inflation.

L-68-849

Figure 12.- Onboard camera photographs.



Time = 8.96 seconds



Time = 9.03 seconds

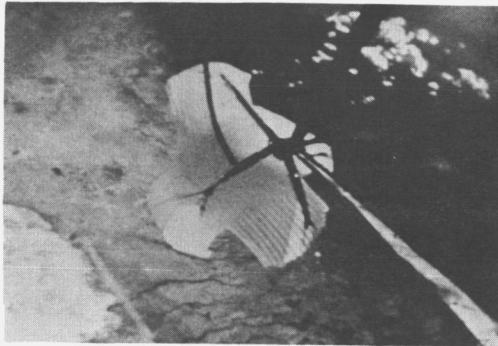


Time = 9.09 seconds

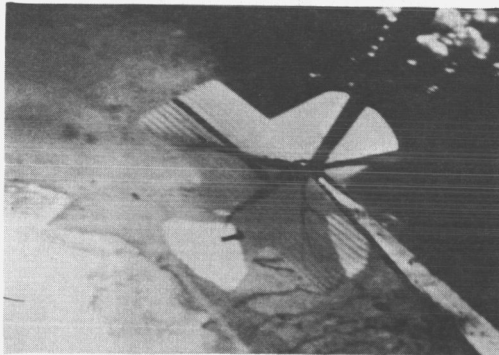
(b) Growth to full inflation.

L-68-850

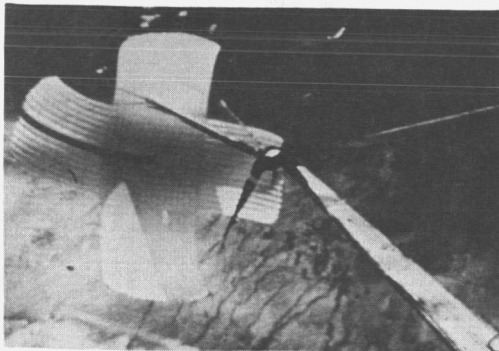
Figure 12.- Continued.



Time = 9.27 seconds



Time = 9.52 seconds



Time = 10.14 seconds

(c) Partial collapse and reinflation.

L-68-851

Figure 12.- Concluded.

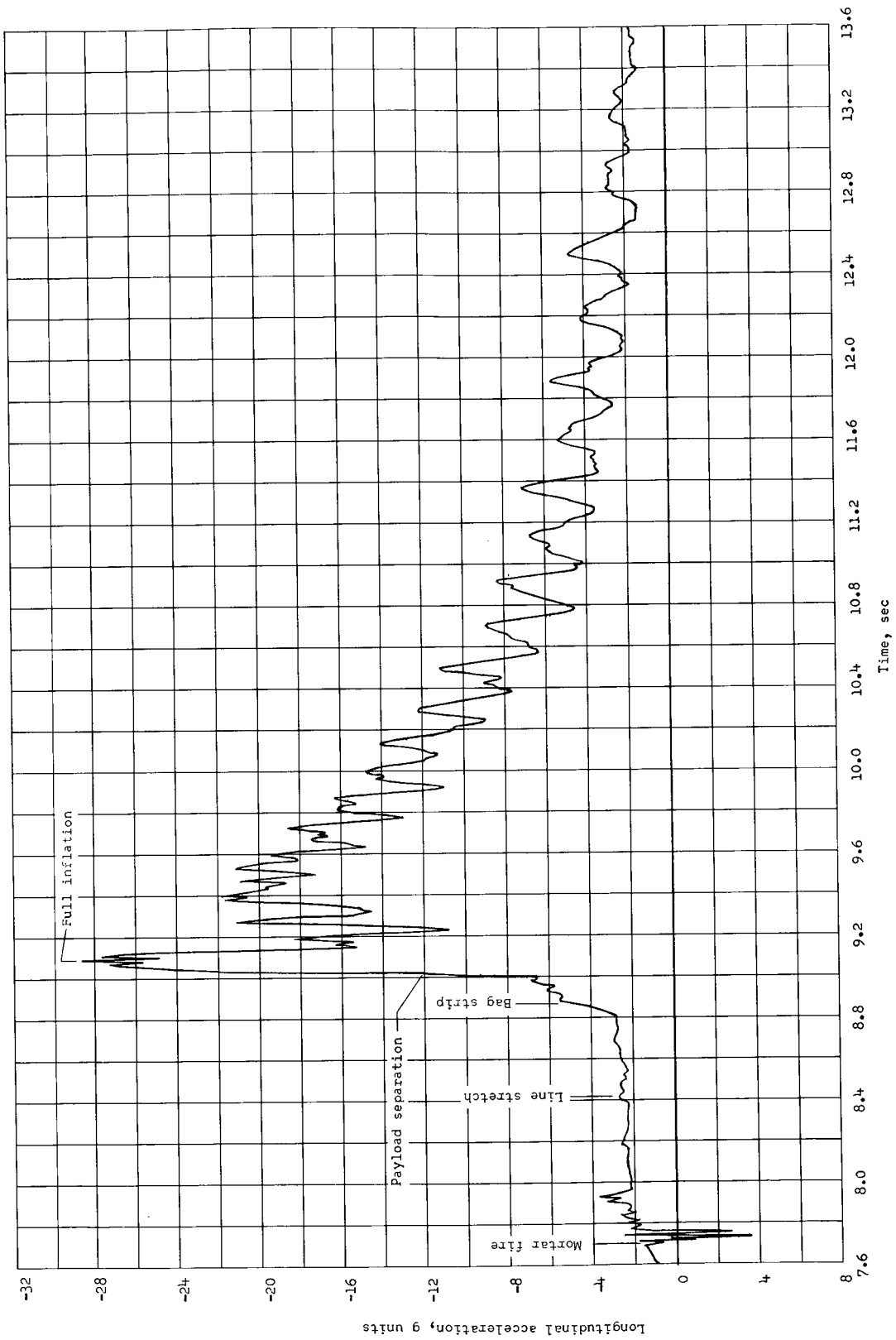


Figure 13.- Variation of longitudinal acceleration with time.

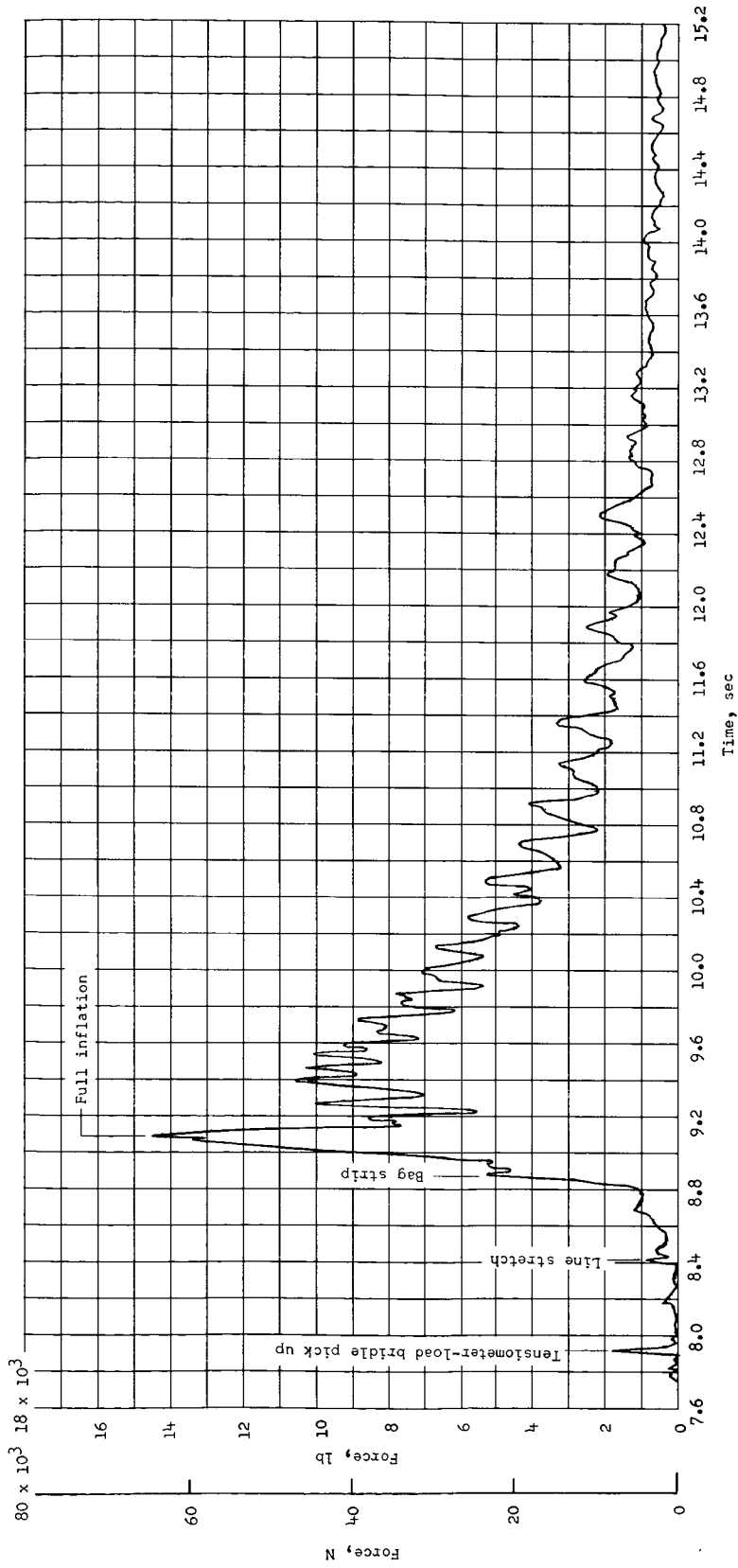


Figure 14.- Variation of tensiometer load with time.

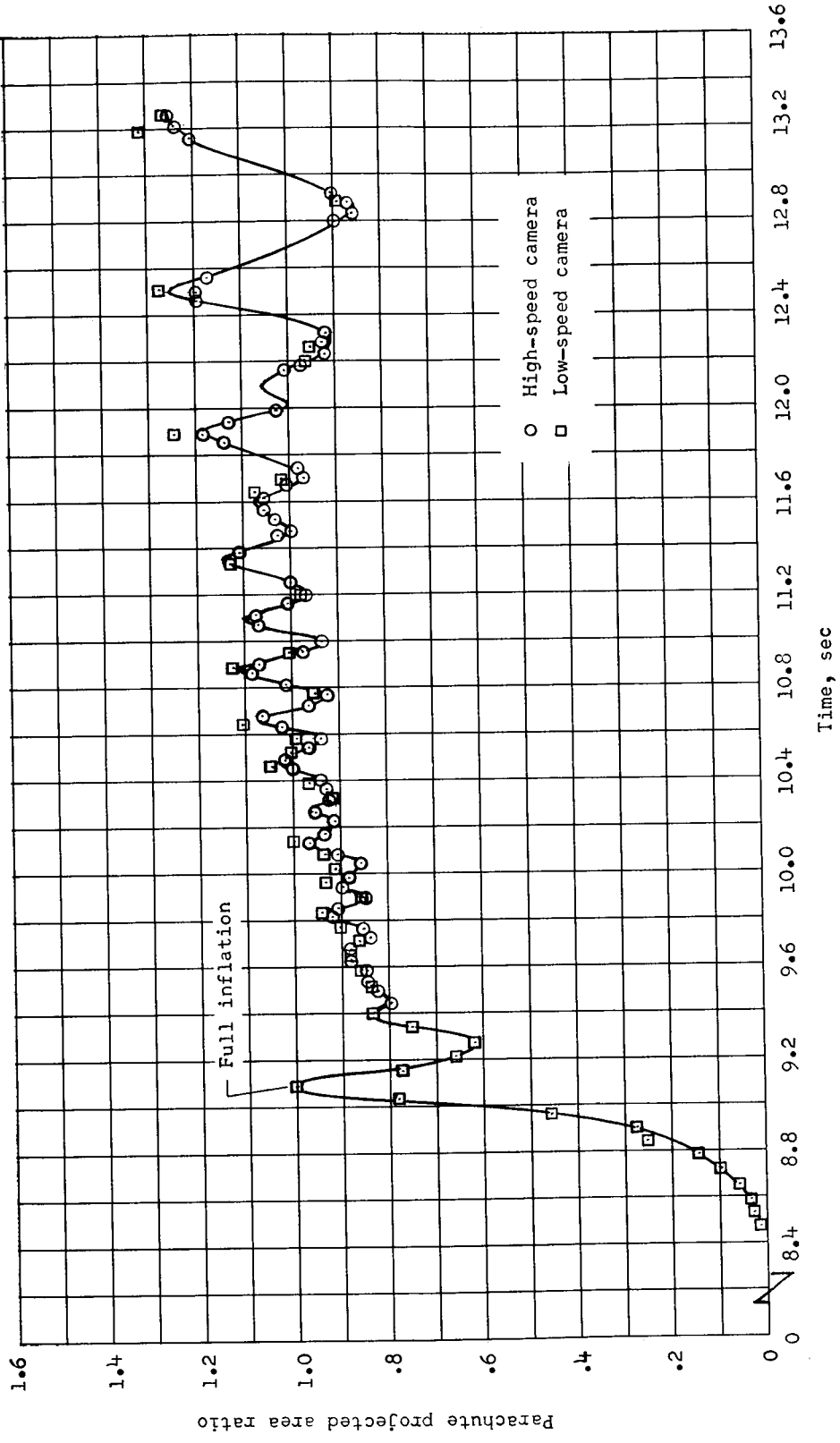


Figure 15.- Variation of parachute projected-area ratio with time.

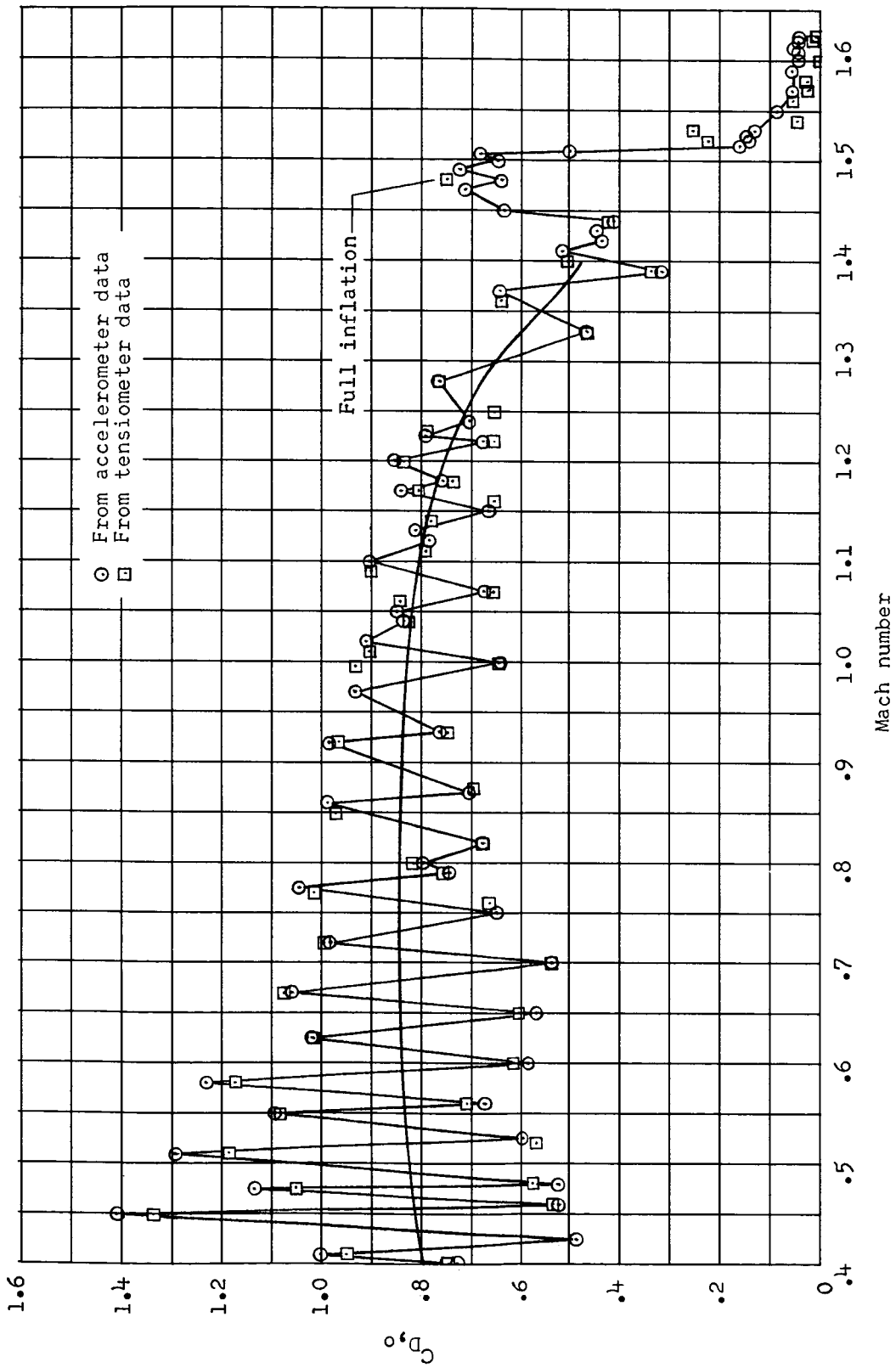


Figure 16.- Variation of parachute drag coefficient with Mach number.

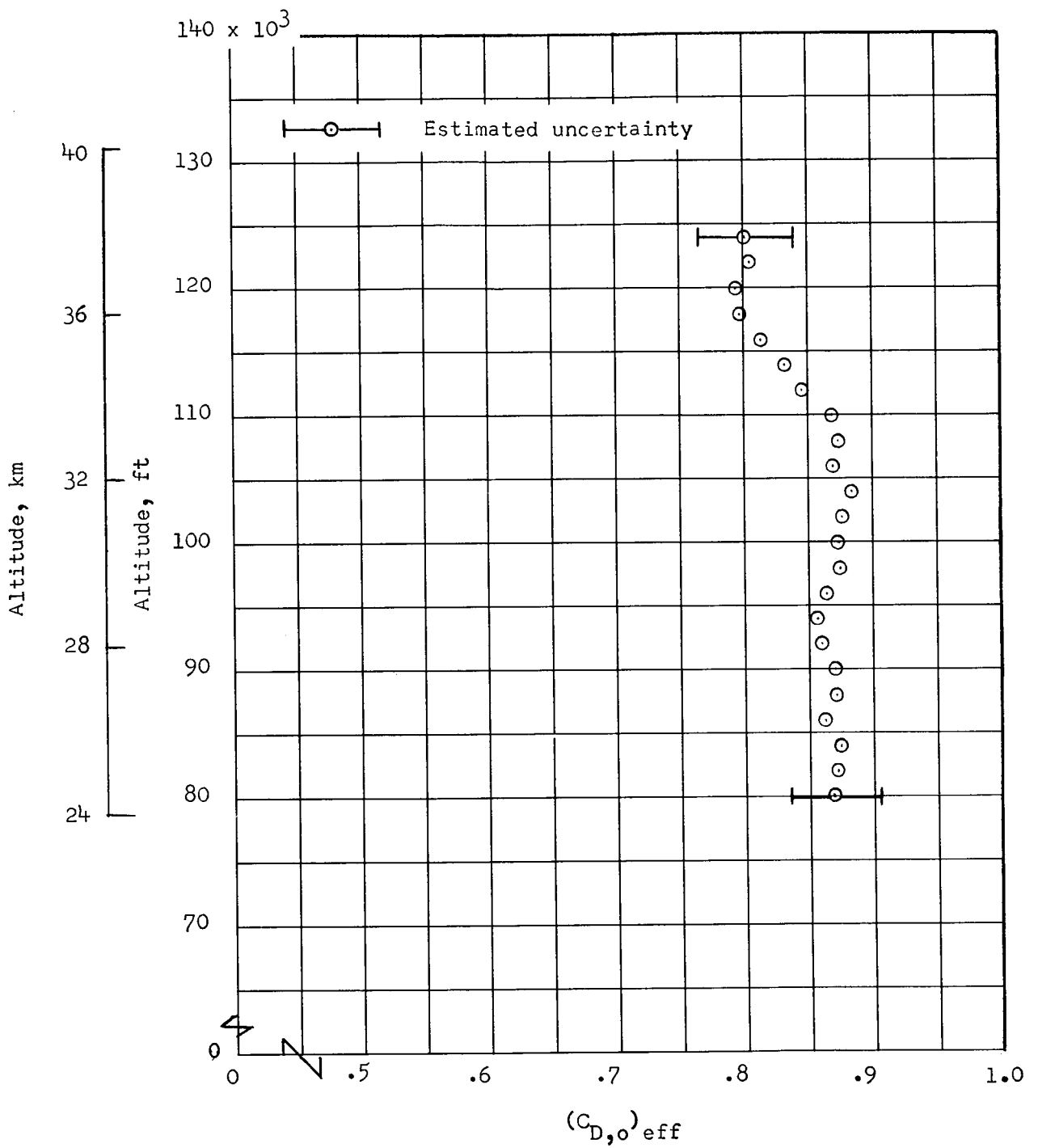


Figure 17.- Variation of effective drag coefficient with altitude.

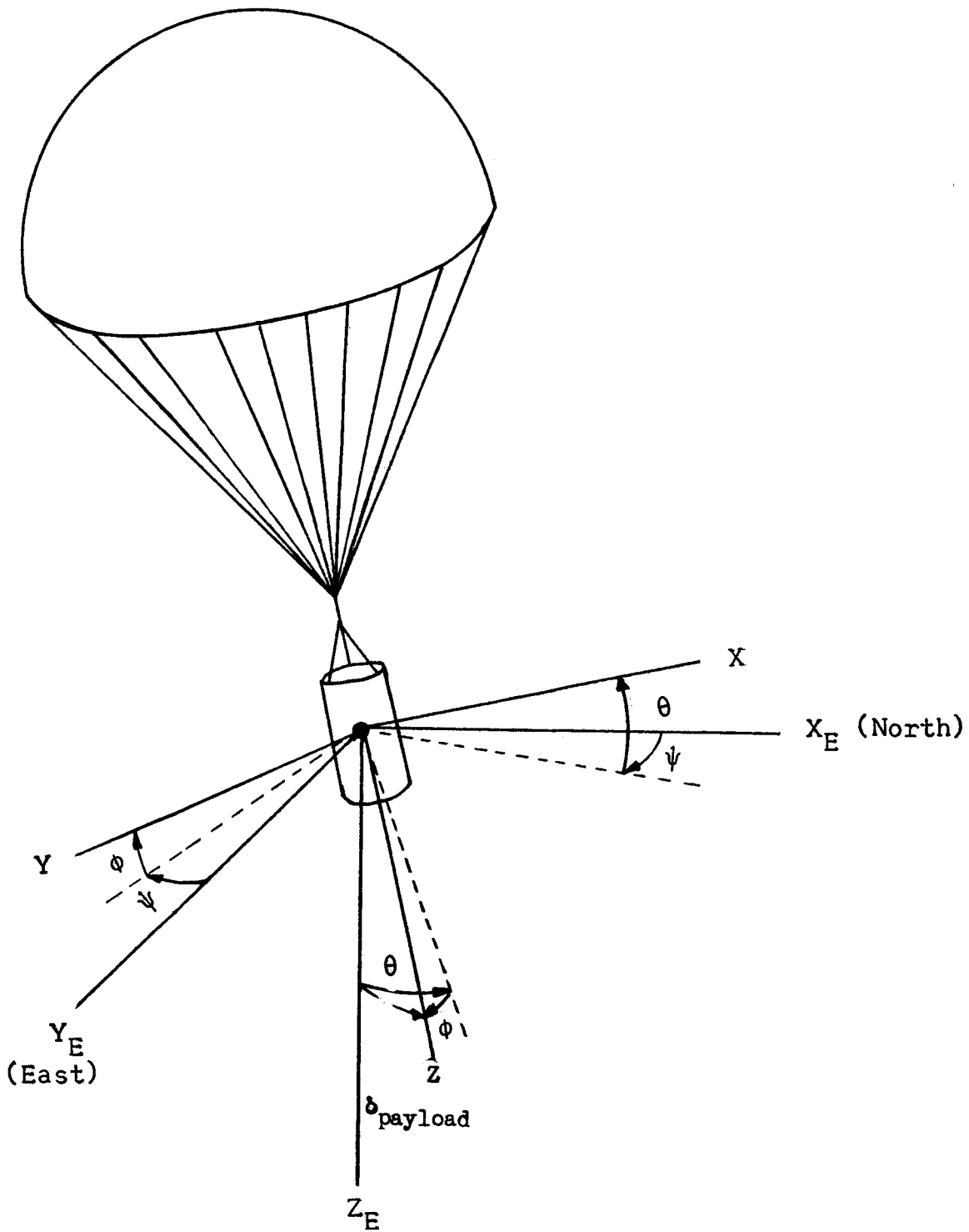


Figure 18.- Body-axis system orientation.

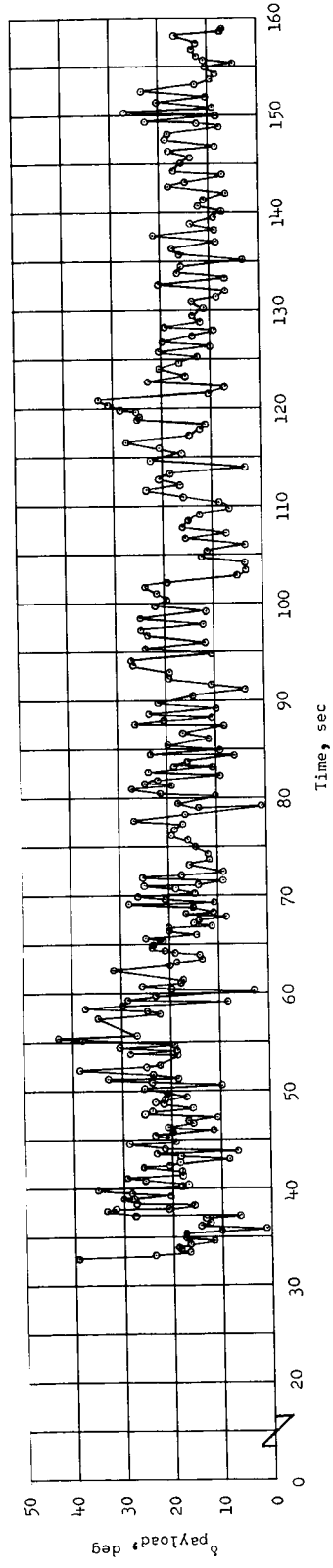
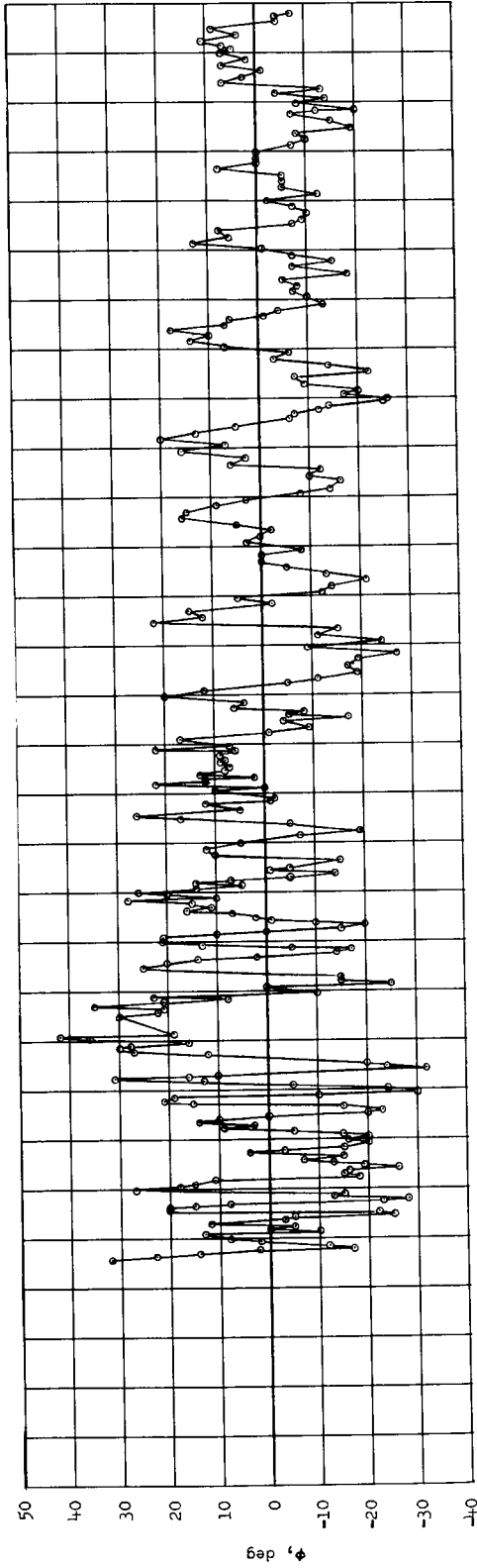
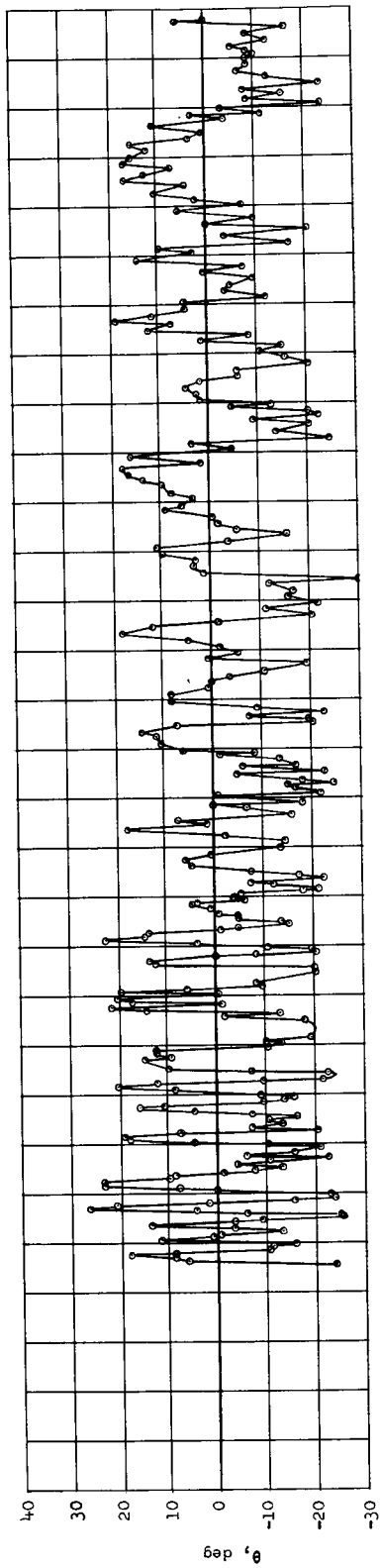


Figure 19.- Variation of θ , ϕ , and δ_{payload} with time.

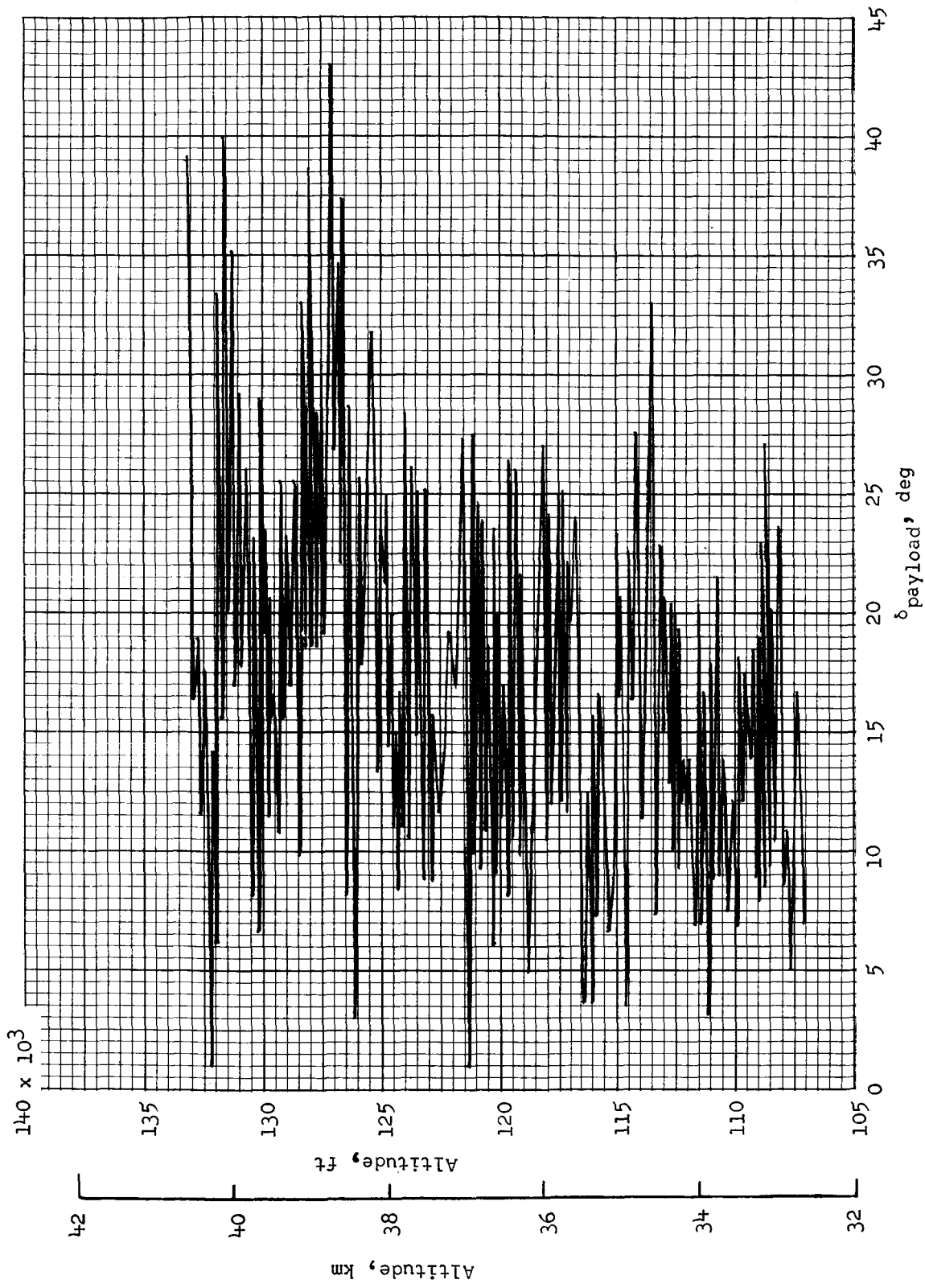


Figure 20.- Variation of δ_{payload} with altitude.

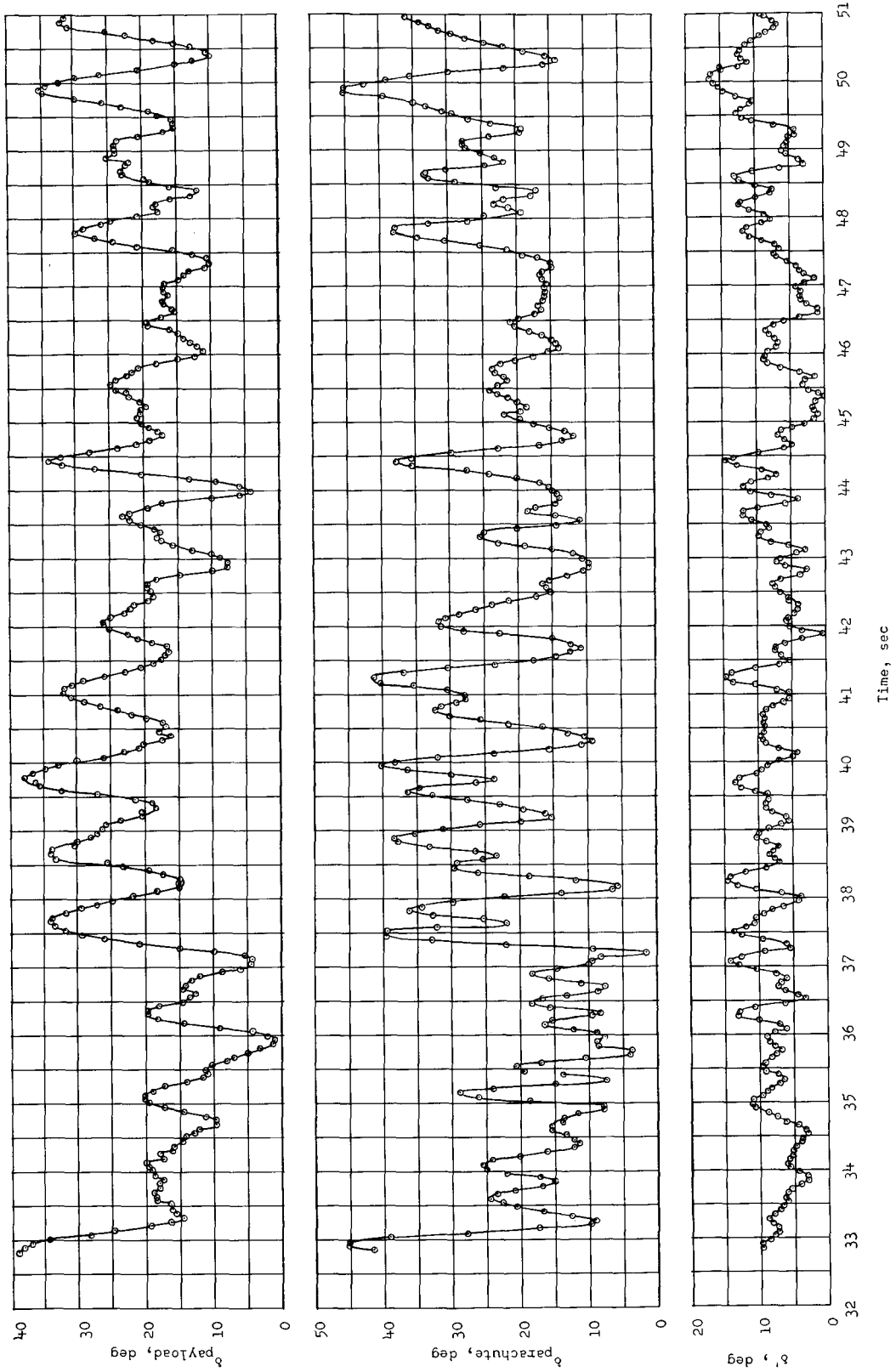


Figure 21.- Variation of $\delta_{\text{parachute}}$, δ_{payload} and δ' with time.

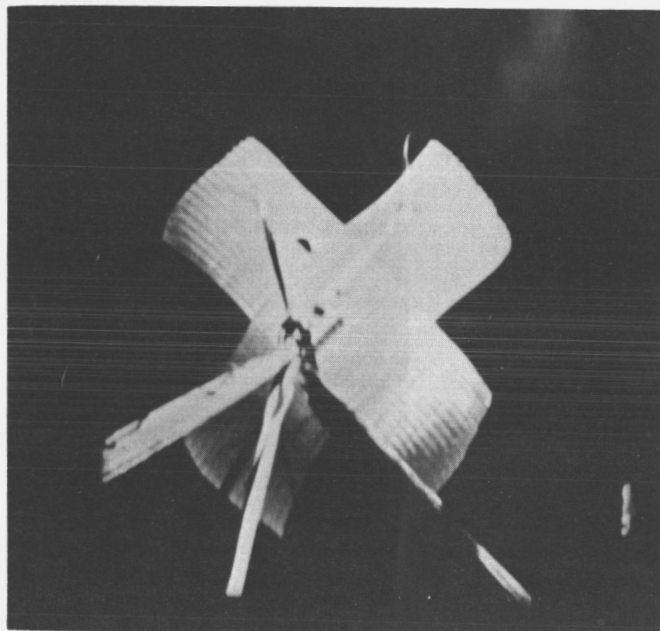


Figure 22.- Photograph of damaged parachute. Time, 30.62 seconds.

L-68-852

A motion-picture film supplement L-985 is available on loan. Requests will be filled in the order received. You will be notified of the approximate date scheduled.

The film (16 mm, 3 min, color, silent) shows parachute deployment, inflation, and payload separation.

Requests for the film should be addressed to

Chief, Photographic Division
NASA Langley Research Center
Langley Station
Hampton, Va. 23365

CUT

Date _____

Please send, on loan, copy of film supplement L-985 to
TM X-1543

Name of organization

Street number

City and State _____ Zip code _____

Attention: Mr. _____

Title _____

Place
Stamp
Here

Chief, Photographic Division
NASA Langley Research Center
Langley Station
Hampton, Va. 23365